Reviews on Advanced Materials and Technologies, 2026, vol. 8, no. 2, pp. 87–116
DOI: 10.17586/2687-0568-2026-8-2-87-116

Extrusion-Based Additive Manufacturing of Polymer-Ceramic Composites and Ceramic Components Using Highly-Filled Feedstocks: A Review

S. Mahboubizadeh [1], A. Jaberi [2,*], E.N. Dresvyanina [2], A. Taherkhani [3], S. Ashouri [3]

[1] Department of Materials Science and Engineering, Islamic Azad University, Science and Research Branch, Tehran, 1477893855, Iran
[2] Institute of Textiles and Fashion, Saint Petersburg State University of Industrial Technologies and Design, Bolshaya Morskaya, 18, Saint Petersburg, 191186, Russia
[3] Department of Engineering, Islamic Azad University, Science and Research Department Branch, Tehran, 1477893855, Iran

Article history

Received April 20, 2026
Received in revised form, May 24, 2026
Accepted May 25, 2026
Available online June 03, 2026

Abstract

Extrusion-based additive manufacturing has emerged as a powerful technique for fabricating polymer-ceramic composites with complex geometries. By enabling layer-by-layer deposition without the need for molds, this process significantly reduces material waste and manufacturing costs, particularly for low-volume and customized production. Among various additive manufacturing technologies, extrusion-based 3D printing methods are widely adopted owing to their cost-effectiveness, design flexibility, and broad material compatibility. These processes typically utilize polymers as binders or matrices, combined with high loadings of ceramic powders and functional additives, where the ceramic phase plays a dominant role in defining the final mechanical, thermal, and functional properties of the component. This review provides a comprehensive overview of extrusion-based additive manufacturing of polymer-ceramic composites. It systematically examines the key material systems, binder formulations, processing routes, post-processing strategies, and critical parameters that govern microstructural development and overall performance.

Keywords: Additive manufacturing; Polymer composites; Ceramic powder; Extrusion; 3D printing

1. INTRODUCTION

Additive manufacturing has emerged as one of the most important advanced fabrication technologies, facilitating the creation of complex geometries tailored to consumer preferences and demands for products and services. Initially, this method was proposed as a means of rapid prototyping. However, with the advent of a wider range of manufacturing techniques, materials and equipment, it is now regarded as a significant production approach [1,2]. Nowadays, manufacturers and researchers routinely produce polymer, ceramic, and metal parts, allowing low-cost production of complex geometries with high design flexibility and very little waste [3,4]. The layer-by-layer nature of additive manufacturing enables precise control over geometry and material distribution, thereby significantly enhancing design flexibility and material efficiency in polymer composite fabrication [5]. It is worth noting that there are few known industries where additive manufacturing has not entered, and it is used in various fields such as aerospace, automotive, biomedical, electronics and construction [6–9]. There are several methods for additive manufacturing of composite parts with polymer binders, including powder-based methods where polymers are applied as a binder or as a layer on top of powders to improve quality. For example, binder jetting is used to produce parts in which the polymer binder is sprayed onto a bed of powder together with other additives [10], or, in the case of the solid based methods, sheet lamination, in which a layered arrangement of sheets with a special component is used [11]. A large number of polymers are also used in processes based on extrusion, in which solid

* Corresponding author: A. Jaberi, e-mail: dzhaberi.a.679@suitd.ru

Table 1. Additive manufacturing process classification.

	Powder based		Slurry based				Bulk solid based	
	Binder jetting		Extrusion based		Photopolymerization based		Sheet lamination methods	
	Powder binder jetting	Slurry binder jetting	Suspension pastes based	Thermoplastic or filament based	Digital light processing (DLP)	Stereolithography (SL)	Laminated object manufacturing (LOM)	Computer aided manufacturing materials (CAM-LEM)
Ref.	[12]	[13]	[14]	[15], [16]	[17]	[18]	[19]	[20]

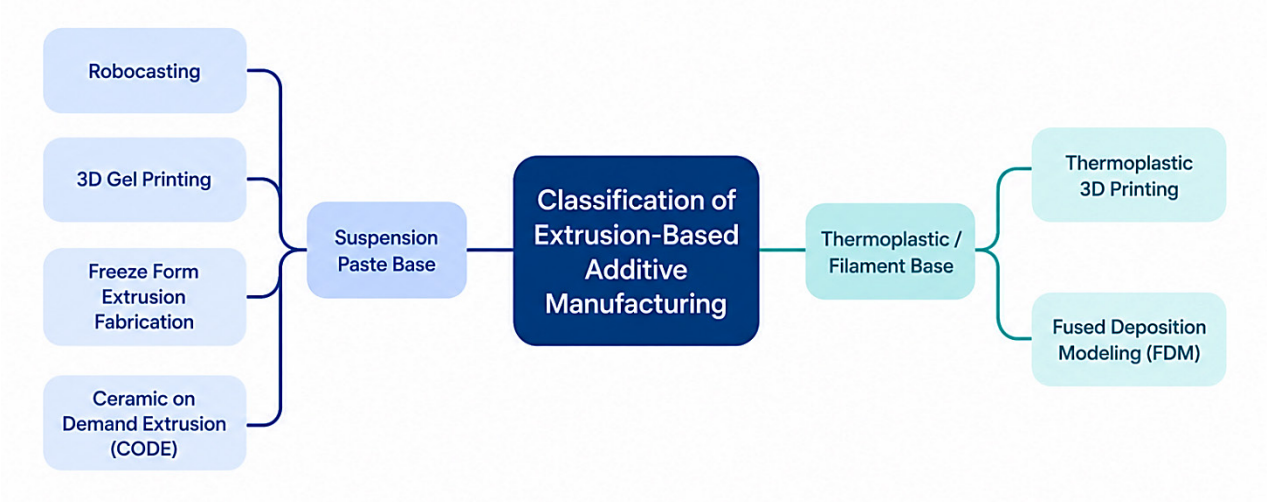

Fig. 1. Classification of extrusion based additive manufacturing.

ceramic or metal particles are placed in a bed of polymers and then extruded either in the form of a paste or in the form of filaments by various extrusion-based 3D printers. Table 1 presents a brief classification of additive manufacturing processes.

In principle, extrusion-based techniques have relative advantages over other proposed methods, including the variety of raw materials used, relatively low manufacturing costs and the ability to customize the manufactured products [21]. The mixing of ceramic or metallic reinforcing materials can play a significant role in shaping the properties of the final product, increasing various strength, chemical and other properties. A brief description of the process is as follows. In extrusion-based 3D printing systems, it is important to create suspension pastes that contain binders together with reinforcements. These reinforcements may take various forms of particles, fibers or platelets [4]. In most cases, to improve printing conditions and increase the amount of ceramic materials in the paste, additives such as plasticizers, surfactants, etc. can be added to the structure after the paste has been formed [13]. In accordance with the methods described in the Figure 1, once the paste or filament has been formed, layer-by-layer construction of the highly filled polymer part can begin [13,22–24].

2. PROCESSING STRATEGIES FOR ACHIEVING FUNCTIONAL 3D-PRINTED COMPOSITE PARTS

Recent studies demonstrate that components fabricated via extrusion-based additive manufacturing (EBAM) can be directly employed as polymer-based composites. However, growing research interest has been directed toward the conversion of these structures into ceramic-based components through polymer-to-ceramic transformation, enabling the transition from polymer-matrix to ceramic-matrix systems. For example, some researchers have been able to convert polymer-derived ceramics into final ceramic parts, after making a polymer composite piece by using a series of secondary processes such as UV irradiation with infrared rays on the manufactured piece, causing the polymer to harden and transform the polymer base into a ceramic structure [25–27]. Most of the new research by some researchers is going towards the construction of parts in which the role of polymers in the structure is more as a binder and the parts made that contain highly loaded polymer together with ceramic or metal compounds [28,29]. After obtaining the green body, an effort is made to extract the polymer in the structure, which has functioned as a binder, from the body of the piece, called

Table 2. Binder systems for ceramic additive manufacturing.

Binder system	Primary components	Typical ceramic loading, vol.%	De-binding method	Key advantages
Aqueous	CMC, HPMC, PVA, PVP, agar, methyl-cellulose	50–60 (up to 58 vol.% optimized; ~ 50 vol.% common in Al_2O_3 slurries)	Thermal (evaporation/pyrolysis)	Environmentally friendly, low toxicity, easy de-binding; good green density in robocasting/DIW
Thermoplastic (wax-based)	Paraffin wax, PE, PP, EVA, PEG, PVB	50–65 (typically 50–60 vol.% in FFF filaments; up to 60 vol.% Al_2O_3)	Thermal or solvent + thermal	High green strength, excellent filament flexibility; suitable for complex FDM/FFF structures
Thermoplastic (catalytic)	POM (polyoxymethylene)	55–65 (commonly ~55–60 vol.%; similar to CIM feedstocks)	Catalytic (HNO_3 vapor)	Rapid de-binding, minimal dimensional distortion; efficient like CIM
UV-curable	Acrylates, methacrylates, photoinitiators	45–60 (up to 60 vol.% in optimized $Al_2O_3/ZrO_2/Si_3N_4$ slurries)	Thermal (after UV-curing)	Instantaneous curing, high resolution, thermoset stability; ideal for SLA/DLP
Bio-based / sustainable	Waste PVB, lignin, starch, PLA	45–60 (typically ~ 50 vol.% in PLA-based filaments)	Thermal / solvent	Low environmental impact, circular economy integration; greener alternative to conventional thermoplastics

de-binding, and finally to move towards a uniform piece of ceramic or porous metal through post-processes. In the subsequent stage, the printed part is subjected to thermal post-processing, such as local melting or sintering, which promotes densification, thereby reducing porosity and significantly enhancing mechanical strength.

This study focuses on extrusion-based additive manufacturing processes incorporating ceramic particles as reinforcing phases. The resulting components can be employed either as polymer-ceramic composites or, through subsequent post-processing, converted into fully ceramic structures that are challenging to fabricate using conventional manufacturing methods.

3. BINDER SYSTEMS IN EXTRUSION-BASED ADDITIVE MANUFACTURING

The binder system represents a critical component in the formulation of highly filled polymer-ceramic feedstocks, governing rheological behavior, printability, green-body integrity, and subsequent de-binding efficiency. In extrusion-based additive manufacturing, binder systems are typically classified into aqueous binders, thermoplastic binders, and photo/UV-curable systems (Table 2).

3.1. Aqueous binder systems

Aqueous binder systems are widely employed in suspension-based extrusion processes such as direct ink writing (DIW), owing to their environmental compatibility and simplified de-binding pathways. These systems typically utilize water-soluble polymers including carboxymethyl cellulose (CMC), hydroxypropyl methylcellulose (HPMC), polyvinyl alcohol (PVA), polyvinylpyrrolidone (PVP), sodium alginate, gelatin, and agar.

These polymers function as rheology modifiers, enabling the development of yield-stress, shear-thinning (pseudoplastic) behavior, which is essential for extrusion and structural recovery after deposition [30,31]. The presence of a finite yield stress ensures shape retention, while shear-thinning facilitates flow under applied stress. Cellulose derivatives such as CMC and HPMC are particularly effective for stabilizing highly concentrated ceramic suspensions, enabling solid loadings up to ~ 55–60 vol.% with relatively low organic content. This significantly improves thermal de-binding efficiency and minimizes defect formation such as cracking and bloating [30,32].

3.2. Thermoplastic binder systems

Thermoplastic binder systems are predominantly used in filament-based EBAM processes, including fused deposition modeling (FDM). These systems are generally multi-component formulations designed to balance melt flow and mechanical stability.

Typical compositions include:

- paraffin wax → reduces melt viscosity;
- backbone polymers (polyethylene (PE), polypropylene (PP), and ethylene-vinyl acetate (EVA)) → provide mechanical integrity.

Advanced systems include polyethylene glycol/polyvinyl butyral (PEG/PVB), which allows partial solvent de-binding through selective extraction of PEG, followed by thermal removal of PVB. This staged removal reduces internal stresses and defect formation [30]. Another important system is polyoxymethylene (POM), which en-

ables catalytic de-binding in nitric acid atmospheres, allowing rapid and uniform binder removal at relatively low temperatures. This approach is well-established in powder injection molding and has been adapted for ceramic additive manufacturing [33].

3.3. Sustainable and bio-based binder systems

Recent developments focus on sustainable binder systems derived from renewable or recycled sources. Modified bio-based carboxymethyl cellulose (CMC) derived from agricultural waste has demonstrated high ceramic loading (~ 58 vol.%) with improved green strength due to enhanced intermolecular interactions [34]. Recycled polyvinyl butyral (PVB) from automotive windshields has also been successfully used as a primary binder in SiC extrusion systems, achieving up to ~ 40% reduction in carbon footprint without compromising performance [35]. Other emerging bio-based binders include starch, lignin, and polylactic acid (PLA). While these materials offer environmental advantages, challenges remain in terms of thermal decomposition behavior, rheological consistency, and process reproducibility [36].

4. CERAMIC MATERIAL SYSTEMS IN EXTRUSION-BASED ADDITIVE MANUFACTURING

The inherent flexibility of EBAM enables the processing of a broad spectrum of ceramic material systems, ranging from conventional oxide ceramics to advanced non-oxide and bioactive compositions. The selection of ceramic type is fundamentally governed by thermodynamic stability, sintering mechanisms, atmosphere sensitivity, and target functional performance. These material classes exhibit distinct processing windows and microstructural evolution pathways during printing and post-processing.

4.1. Oxide ceramics

Oxide ceramics are the most extensively investigated class in EBAM due to their chemical stability in ambient atmospheres, relatively well-established powder processing routes, and predictable sintering behavior.

Among them, alumina (Al_2O_3) and yttria-stabilized zirconia (ZrO_2, particularly 3Y-TZP) are the most widely utilized. Alumina offers high hardness, wear resistance, and thermal stability, whereas zirconia provides superior fracture toughness due to the transformation toughening mechanism (tetragonal → monoclinic phase transformation) [37,38].

In EBAM processes such as direct ink writing (DIW), these materials can achieve relative densities exceeding 95–99% after optimized sintering, provided that high solid loading (> 50 vol.%) and homogeneous particle dispersion are achieved. Rheological optimization is critical to suppress defects such as interlayer delamination and anisotropic shrinkage [39].

Functional oxide ceramics such as barium titanate ($BaTiO_3$) have gained increasing attention for piezoelectric and dielectric applications. Recent studies have demonstrated that EBAM-processed $BaTiO_3$ components can achieve densities above ~ 96%, with preserved ferroelectric properties, when processed via optimized aqueous gel systems and controlled thermal cycles [40]. However, challenges remain in controlling grain growth and domain orientation during sintering, which directly influence dielectric and piezoelectric performance. Figure 2 shows the fundamental ceramic material variants commonly used in extrusion-based 3D printing systems.

4.2. Non-oxide ceramics

Non-oxide ceramics, including silicon carbide (SiC), silicon nitride (Si_3N_4), and boron carbide (B_4C), are characterized by exceptional mechanical strength, thermal conductivity, and chemical resistance, making them suitable for extreme environments. However, their processing via EBAM is significantly more complex due to oxidation sensitivity, covalent bonding nature, and limited self-diffusion during sintering.

These materials typically require:

- controlled (inert or reducing) atmospheres to prevent oxidation during high-temperature processing;
- sintering additives (e.g., Y_2O_3, Al_2O_3 for Si_3N_4) to promote liquid-phase sintering and densification.

For instance, Si_3N_4 densification relies on transient liquid phases formed by oxide additives, which facilitate particle rearrangement and solution–reprecipitation mechanisms [41].

In the case of silicon carbide, pressure‑less sintering often requires boron and carbon additives to enhance densification kinetics. Achieving high density (> 95%) remains challenging due to grain boundary diffusion limitations [42].

Advanced non-oxide systems such as ultra-high temperature ceramics (UHTCs)—including zirconium diboride (ZrB_2) and titanium diboride (TiB_2)—have been successfully processed using EBAM techniques such as robocasting and colloidal direct extrusion (CODE). These materials exhibit melting points above 3000 °C, making them suitable for aerospace and hypersonic applications [43].

Recent studies report relative densities exceeding ~ 95%, with tailored microstructures achieved through the incorporation of secondary phases (e.g., SiC) to improve fracture toughness and oxidation resistance [42]. Nevertheless, controlling crack formation during drying and sintering remains a key challenge due to their intrinsic brittleness and high elastic modulus.

Fig. 2. Ceramic material system in extrusion-based additive manufacturing.

4.3. Bioceramics

Bioceramics represent a distinct class of materials in EBAM, primarily used for bone tissue engineering and regenerative medicine. Common compositions include:

- hydroxyapatite (HA);
- tricalcium phosphate (TCP);
- bioactive glass (e.g., 45S5-NovaMin© calcium sodium phosphosilicate bio‑glass);
- calcium silicates•(e.g., akermanite, wollastonite).

These materials are typically fabricated as highly porous 3D scaffolds, where porosity (50–90%) and interconnected pore architecture are critical for cell infiltration, vascularization, and nutrient transport [44].

A central challenge in bio‑ceramic processing is the trade-off between porosity and mechanical strength. While high porosity enhances biological performance, it significantly reduces compressive strength and structural reliability. EBAM enables precise control over pore geometry and gradient architectures, allowing partial mitigation of this trade-off through topology optimization and hierarchical structuring.

Additionally, the bioactivity of these materials is strongly influenced by surface chemistry, ion release kinetics, and phase composition. For example, HA provides excellent biocompatibility but relatively low resorption rates, whereas TCP exhibits faster biodegradation. Composite or multiphase systems are often employed to balance these properties [45].

5. EXTRUSION 3D PRINTING OF POLYMER-CERAMIC COMPOSITES

In extrusion-based additive manufacturing, a slurry or paste is prepared by mixing a polymer (acting as a matrix or binder), ceramic particles (as reinforcement), along with other necessary additives. This mixture is then extruded through a nozzle to fabricate the desired part [46,47]. Different post-processing routes may subsequently be applied depending on the intended final application. As illustrated in the Figure 3, the manufactured parts may be used directly as polymer composite components, or they can undergo curing via exposure to IR or UV radiation when using photosensitive or IR-curable polymers. Alternatively, post-processing involving de‑binding of the polymer and subsequent sintering can be applied to convert the ceramic compounds into a strong, dense final ceramic part.

Figure 4 shows different nozzles of extrusion-based 3D printers. In pneumatic extrusion, a continuous pressure is applied to the paste inside the extrusion chamber, causing a continuous ejection of the paste and its application to the platform. In piston mode, the piston applies a uniform mechanical pressure to the paste inside the nozzle. This mode has the ability to apply more force than the pneumatic mode and is therefore suitable for printing very high viscosity pastes [48,49]. And in the screw mode, after entering the nozzle, the paste hits the spiral impellers, where the paste is guided by the torsional flow generated along the extrusion nozzle to the end of the nozzle outlet

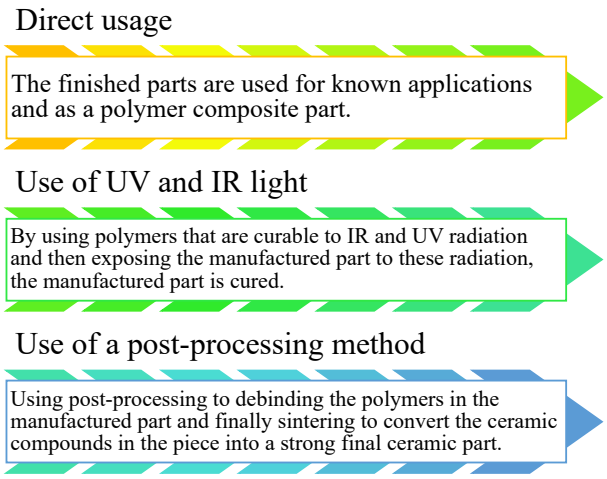

Fig. 3. Classification of processing routes for converting extrusion-based 3D printed green bodies into final parts, categorized based on technological process pathways and the resulting final-state products, including polymer–ceramic composites and fully ceramic structures.

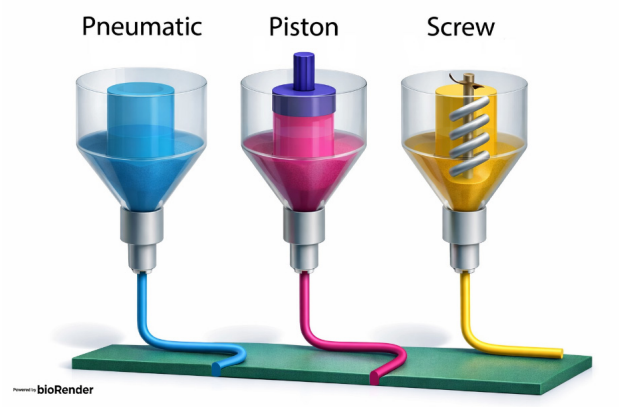

Fig. 4. Three common extrusion mechanisms in extrusion-based 3D printing: (left) pneumatic extrusion driven by air pressure; (middle) piston extrusion using mechanical force; and (right) screw extrusion with a rotating auger.

and is applied to the surface of the platform. This leads to the elimination of material selection limitations for 3D printing technology and also helps to mix different components in the paste with low or high viscosity [50]. Finally, it is important that the choice of each of these nozzles is directly related to the type of raw material used and its composition, for example, if paste is used, its rheology is important, and if filament is used for extrusion, the diameter of the filament and the amount of melt required to get the filament out of the nozzle and then its ability to melt are important.

One of the key aspects of this manufacturing process is to ensure an appropriate number of ceramic particles are incorporated into the polymer matrix. This involves ensuring that the quantity of solid particles within the polymer is substantial, and that their distribution within the polymer matrix is homogeneous. Furthermore, the viscosity of the paste is precisely calibrated to eliminate any potential issues not only during the extrusion process, but also during the subsequent manufacturing of the part [51]. Most of the suspension pastes used in extrusion-based 3D printers have non-Newtonian fluid behavior, which is often divided into dilatant and pseudoplastic fluids. In paste with dilatant behavior, by applying force to the paste, the paste becomes rigid. and the resistance shows that this is a problem in the discussion of using extrusion and it causes the paste to come out of the nozzle with difficulty and after the force is removed, it becomes loose and cannot have the desired layered structure to manufacture the part. In pseudoplastic pastes, viscosity decreases under shear stress, facilitating smooth extrusion through the nozzle, while rapid viscosity recovery after deposition helps maintain the printed geometry and the layered construction of parts by extrusion. However, in the case of pastes with pseudoplastic behavior, the force reduces the fluidity of the paste, which hardens again when the force is removed, thus preventing the paste from exiting the nozzle and making it possible to build up the parts in layers by hardening the paste [52].

On the other hand, polymer-based pastes behave as viscoelastic materials. These types of viscoelastic materials need to have a suitable tensile strength in addition to being fitted to the model for yield pseudoplastic fluid [53] and most suitable tensile strength for extrusion are in the range of 100–1000 Pa [54–56]. For this purpose, polymer pastes with increased solid ceramic particle content and higher concentrations of polymer binders (e.g., methyl cellulose [57], polyvinylpyrrolidone (PVP) [58], and polyethyleneimine (PEI) [59]) can be prepared to provide the required viscoelastic properties. In this regard, two primary categories of extrusion-based 3D printing processes are of interest for fabricating polymer-ceramic composites. The first involves suspension paste-based extrusion technologies, in which a low-viscosity or yield-pseudoplastic paste is prepared as a suspension containing ceramic particles, a solvent (typically water or organic solvents), a polymer binder, and other additives. This approach operates at room temperature without requiring melting of the paste, enabling higher ceramic loadings (often > 50 vol.%) and simpler de-binding. The second category encompasses filament- or thermoplastic-based extrusion processes, where ceramic particles are dispersed within a thermoplastic polymer matrix to form either pre-extruded filaments or granules/pellets. These feedstocks are then fed into a heated extruder, melted, and deposited layer by layer. Although this method typically involves lower ceramic loadings compared to suspensions and requires thermal management during printing, it offers excellent process stability, compatibility with commercial fused deposition modeling/fused filament fabrication (FDM/FFF) printers, and the ability to produce complex geometries with good green-body handling. Both approaches are followed by

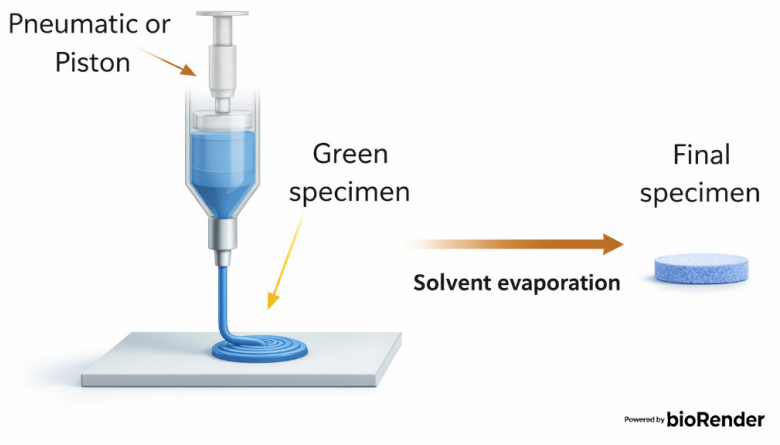

Fig. 5. Schematic of suspension paste extrusion 3D printing.

appropriate post-processing (curing, de-binding, and/or sintering) depending on whether the final part is intended as a polymer-ceramic composite or a dense monolithic ceramic component; they will be examined in detail in the following sections.

5.1. Extrusion additive manufacturing based on suspension pastes

The advantage of this method over other methods of producing polymer composites is the use of more ceramic particles within the polymer matrix. In this method, the formation of a suspension leads to a reduction in the use of organic materials and polymers. Finally, the de-binding process of the polymer within the structure becomes easier, which, in addition to ease of manufacture, also leads to a reduction in defects in the part. For this reason, most of the extrusion-based processes developed emphasize the use of suspension paste. Figure 5 shows a schematic of the additive manufacturing process for the production of suspension paste containing ceramic particles using extrusion-based 3D printers.

Among the challenges of this method are the direct effect of the shape, size and surface morphology of the particles, including surface roughness, on the behavior of the paste prepared; on the other hand, the stabilization of the suspension to obtain a homogeneous mixture with reinforcing ceramic particles is important in the context of polymer, which depends on the precise control of the paste formulation and other printing parameters to obtain the desired final product [60]. In the following, the different methods of the 3D printing subset of suspension paste extrusion will be examined.

5.1.1. Robocasting

Robocasting (RC), another name for direct ink writing (DIW), is based on the extrusion of a polymer-based paste, where the resulting paste acts as a binder and, if ceramic particles are added, various additives can be used to facilitate the printing process. These additives control the rheology and other properties of the paste [61–63]. Depending on the nozzle used for this process, the filament diameter of the materials exiting the robocasting nozzle is in the range of 200–800 μm. Another important consideration is how these exiting filaments are deposited onto the platform, so that when integrated samples are produced, the distance between the filaments that make up a layer is considered to be zero, preventing sample distortion [64]. However, the distance between the deposited filaments on the platform is considered a positive factor in the manufacture of porous ceramics [64]. Wahl et al. [65] prepared a suspension paste containing silicon carbide particles and carbon and then produced a SiC/C green-body using RC. They then used reaction sintering and liquid silicon infiltrate (LSI) to produce the final part, where the density of the final part and its four-point flexural strength were measured to be 98% and 224 MPa respectively. A schematic of the DIW is shown in Figure 6.

Adequate dispersion of the solid particles is essential to obtain a well homogenized suspension. In addition, small amounts of other additives such as viscosifiers, plasticizers, thickeners in the range of 0–5 wt.% could be used to increase the stability of the suspension and provide rheological properties [66,67]. Although some problems have been observed in the manufacture of parts via robocasting, including residual porosity, drying cracks, and delamination between filaments (particularly in non-optimized printing directions), recent studies have introduced effective strategies to mitigate these issues through advanced ink formulations and optimized printing parameters. Notably, Feilden et al. [68] demonstrated that by employing a robust hydrogel-based ink (Pluronic F-127) with high solid loading and carefully controlled rheological properties, dense monolithic alumina and SiC parts with excellent interlayer bonding and flexural strengths of

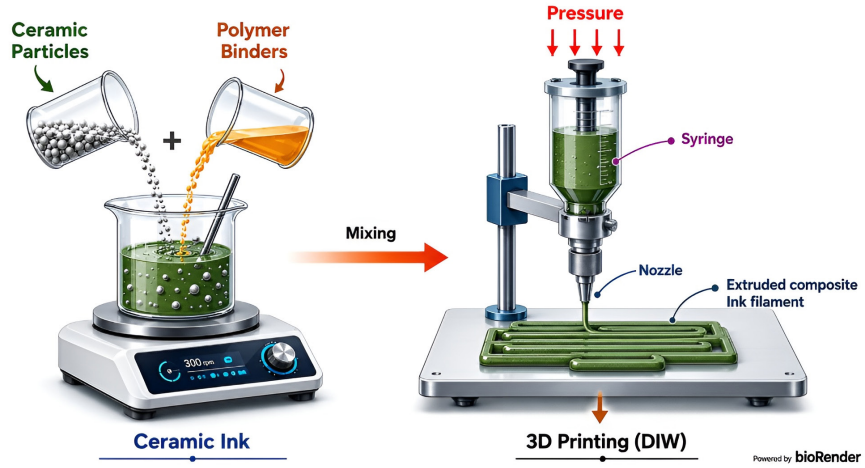

Fig. 6. Schematic representation of ceramic fabrication via direct ink writing (DIW).

Table 3. Mechanical properties of robocast alumina parts after sintering.

AM process	Ceramic material	Polymer material	Ceramic powder loading, vol.%	Density, %		Flexural strength, MPa	Ref.
				Green	Final		
Robocasting (DIW)	Al_2O_3	Carrageenan	56	—	97.6	250.86	[72]
		Ammonium polyacrylate	55	—	98	156.6 ± 17.5	[39]
		Pluronic F-127	36	—	97	230	[68]

230 MPa and 300 MPa, respectively, can be successfully fabricated.DIW was used to produce a part made of SiC and carbon fibers by Xia et al. [69]. The final part had a porosity of 30.9–34.8%. The ultimate strength was measured in the range of 84–123 MPa. In addition, its fracture toughness was measured to be approximately 1.46–2.71 MPa·$m^{1/2}$. Costakis et al. [56] prepared an aqueous suspension paste containing ceramic boron carbide (B_4C) particles and polyethyleneimine (PEI), where the sample containing 2.7 vol.% WC has a density of 2.88 g/cm^3 and a tensile strength of 43 MPa. They showed that the probability of cracking increased with increasing solid particles. Kemp et al. [70] fabricated a ceramic composite part from polysiloxane reinforced with hexagonal boron nitride (hBN) using DIW, where the flexural strength of the parts obtained was approximately 56.4 MPa and with a microhardness of 111.4 HV2, indicating lower porosity and more uniform pore distribution. In another study, Shao et al. [71] produced glass frameworks by forming a $CaSiO_3$-based paste (4.5 grams of ceramic powder with 4.0 grams of polyvinyl alcohol (PVA)), applying it to a DIW platform, and sintering to produce a 60% porosity part with a compressive strength between 48 and 88 MPa. Table 3 presents an analysis of the literature investigating the research conducted on the additive manufacturing of alumina-containing parts. These methods have used heat treatment for de-binding and sintering to obtain alumina parts.

By optimizing the deposition pattern, suitable network structures can be created to achieve better mechanical performance. Other parameters affecting the rheology of composite pastes include the effect of the morphology of the particles added on the viscosity and the loading of the ceramic particles in the past [22]. Compounding significantly affects the rheological behavior of the feedstock. In general, increasing the volume fraction of ceramic particles leads to an increase in viscosity due to intensified hydrodynamic interactions and particle–particle contacts within the suspension. Excessively high viscosity may reduce flowability and impair printability during extrusion-based additive manufacturing. The mechanical properties of the parts produced by this method are also directly influenced by the manufacturing conditions of the samples as well as the parameters of the molded paste, so that if the molded paste has a suitable printability and the additives and solvents in it are optimal during the 3D printing process, it will find the least defects and porosity. On the other hand, if the distance between the nozzle and the substrate as well as the speed of the nozzle movement are optimal, it will lead to a high quality printing of the paste layers on top of each other, eliminating problems such as lack of filling and the part will be printed with high quality [22,73]. According to some research, there is a type of robocasting in which the paste used for 3D printing has a lower viscosity than robocasting [74,75] which are also included in the field of extrusion free form (EFF), but still found in a

separate category. In principle, EFF can be applied to all methods based on extrusion, and new methods that have many similarities to other known methods, but the difference is the parts seen in them are mentioned under the title of extrusion. This type of additive manufacturing method will be investigated below [74,75].

For instance, Gomez et al. [76] fabricated a silicon carbide part using EFF 3D printing. The final piece formed with porosity about 65–85% after SPS sintering. Zhang et al. [77] fabricated a part containing silicon carbide along with carbon black and chopped carbon fibers where the final composite piece had a 3-point bending strength of 300 MPa. McLainn et al. [78] prepared a suspension using ceramic precursors along with 45 wt.% chopped carbon fibers and 10 wt.% carbon black, and using EFF on a platform based on pyrolysis. The mechanical properties of the resulting composite parts were comparable to those reported in previous studies on alumina-containing composites fabricated by similar extrusion-based methods. The de-binding and sintering processes were also used in this preparation method for achieving final desirable specimen.

5.1.2. Freeze-form extrusion fabrication

The paste formed in this process is a water-based suspension containing ceramic particles or a colloidal gel, which is modified after preparation. Of course the extrusion method is modified so that the desired paste is applied to the substrate after extrusion. After deposition and formation of a layer, it is frozen [78]. Basically, the paste generated from the computer-aided design (CAD) model is printed in a controlled freezing environment, typically between 0 °C and −20 °C, depending on factors such as the solvent freezing point, slurry rheology, ceramic solid loading, and the required dimensional stability during deposition. After fabrication of the composite sample, the structural water is removed through a freeze-drying process, in which the selected drying temperature and pressure are determined by the sublimation behavior of ice, pore preservation requirements, and prevention of structural collapse or cracking during solvent removal [79,80]. The advantages of this method include the production of large parts, the reduction of the use of polymer binders for the production of high-density parts, and the reduction of waste, which is not only considered to be an environmentally friendly method. The mechanical properties of the parts are also important due to the high density of the parts manufactured [80].

One of the primary limitations of freeze-form extrusion fabrication (FEF) is its relatively low dimensional accuracy compared with other extrusion-based additive manufacturing techniques. Surface irregularities and geometric distortion are mainly attributed to ice-crystal growth, solvent sublimation, and anisotropic shrinkage during freeze-drying [38]. Reported dimensional deviations in FEF-fabricated ceramic parts generally range from approximately 1–5%, whereas optimized robocasting and filament-based extrusion methods commonly achieve deviations below 1–2%. The severity of these defects strongly depends on slurry rheology, freezing rate, solid loading, and freeze-drying conditions [78].

The effective point of this processes is the control of the viscosity of the extruded slurry in such a way that the control of the rheological properties of the paste and the slurry is a determining factor for the properties of the final product in this process [81]**.** Applications of this process include the production of functionally graded materials (FGM), such as alumina oxide parts, and the use of a polymer such as methyl cellulose to form metal parts [82–84]. In a study using FEF, Ghazanfari et al. [75] successfully fabricated alumina components with a relative density of up to 98% after sintering, exhibiting flexural strengths in the range of approximately 200–350 MPa.

5.1.3. 3D gel printing

3D gel printing is one of the new additive manufacturing methods for producing complex composite parts, so it's a relatively modern process that evolved from both gel casting and 3D printing. In this process, the first step is to prepare a gel-like suspension of polymer and other ceramic fillers; the resulting polymer network is responsible for the retention and distribution of the ceramic particles during the printing process, then the resulting gel paste is extruded into the desired part shape, and finally, through processes such as curing, the final three-dimensional structure is created [85–87]. It should be noted that in this process, the gel rheology, curing mechanism and printing machine parameters have led to the construction of polymer composite parts with better mechanical and functional properties [85,86]. In one study, they investigated the process of 3D gel printing for the production of raw parts relevant to the gelling process of 2-hydroxyethyl methacrylate (HEMA) [85]. A schematic of the 3D gel printing process is shown in Figure 7.

The advantages of this method include the ability to produce samples of large size and at high speed. This method can be used for all ceramic particles. The cost of the equipment used in this method and the preparation of the raw materials for the production of the parts is low. It is also possible to mention the possibility of manufacturing composite parts with complex geometries and shapes, in addition to the possibility of manufacturing polymer composite parts with different compounds with high efficiency, and finally the versatility in all types of thermosets, thermoplastic and hydrogel polymer fields [87,88].

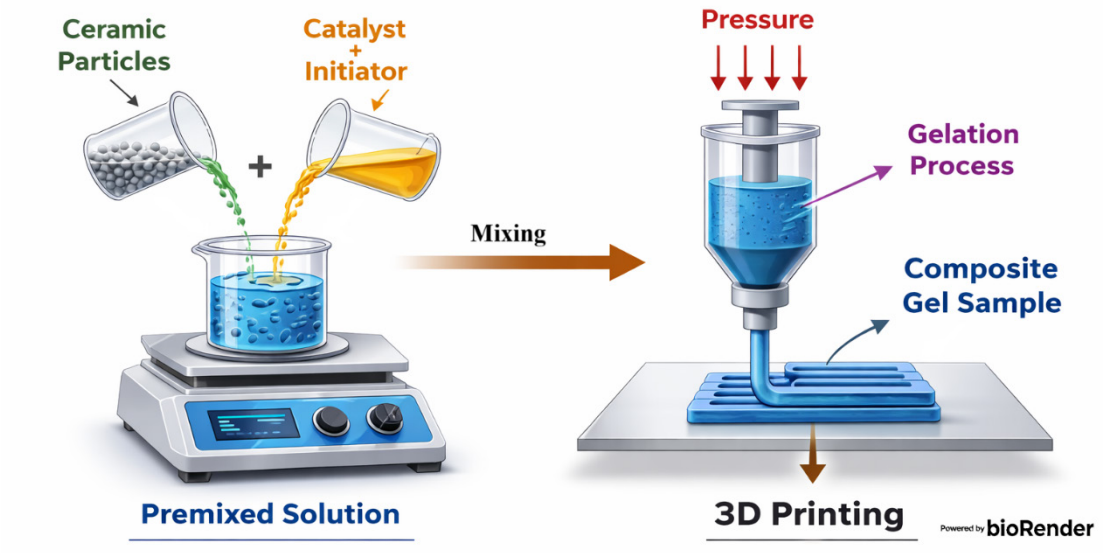

Fig. 7. Schematic of additive manufacturing process by 3D gel printing.

5.1.4. Ceramic on demand extrusion

This method is an additive manufacturing process based on extrusion, in which an infrared radiation process is used to manufacture the final parts from the print, where the final piece is not a composite part, but an all-ceramic piece with a high density and strength [89–91]. The process of manufacturing parts in this way first involves extrusion printing of the samples, in which the suspension paste produced contains a much smaller amount of binder in the presence of water solvent, and this paste should be able to be printed at room temperature [90]. The printing process in this method differs from conventional extrusion techniques. After each layer is deposited, the structure is continuously immersed in an oily fluid prior to the next layer deposition. This controlled immersion regulates the drying rate and effectively prevents uneven drying and capillary crack formation. Subsequently, infrared radiation is applied to partially and uniformly cure the green body. The combination of low binder content and the elimination of capillary cracks during the controlled drying process significantly enhances the strength of the molded part [91]. By determining the control parameters of the extrusion process and drying, it is possible to obtain parts with a density close to the theoretical value and with high mechanical properties. The applications of this method can be used to produce parts with complex compositions and geometries that have good density and strength. The most common applications today are compact heat exchangers, power generation systems and sensors [89–91]. A schematic of the additive manufacturing process using the ceramic on demand extrusion (CODE) method is shown in the Figure 8.

Yield-pseudoplastic rheology gives the suspension structural integrity up to its yield stress, followed by shear-thinning behavior [92,93]. This behavior is critical for the ink as it must flow through the die due to the high shear environment and maintain its shape after being applied to a substrate. McMillen et al. [94] used CODE to produce ultra-high temperature ceramics from ZrB_2 which has a density of 99% and PVA binder along with other nitride and carbide additives. This technique is a pioneering method suitable for the production of parts with complex shapes [94].

5.2. Extrusion additive manufacturing based on thermoplastic or filament

Extrusion printing of composite parts based on thermoplastic and filament is a method that is a category of additive manufacturing methods of ceramics, which includes two techniques, fused deposition modelling (FDM) [15] and thermoplastic 3D printing [16]. The steps involved in manufacturing parts using these methods involve extrud-

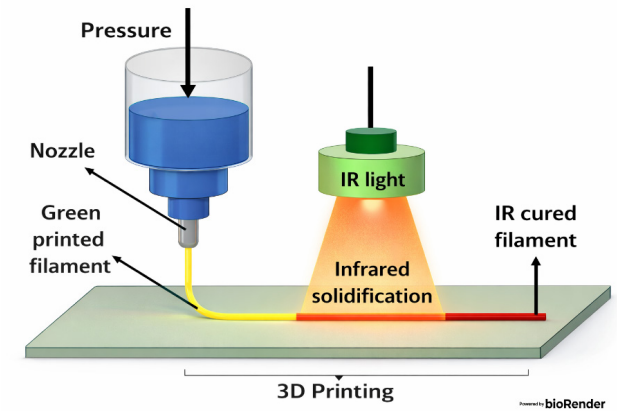

Fig. 8. Method of fabrication of ceramic parts using IR curing CODE process.

ing a mixture of ceramic and polymer materials through a 3D printer, layer by layer [95]. The polymer used in the thermoplastic paste, when mixed with ceramic particles or other additives, can be fed directly into the printer's extruder and start making 3D parts, or the mixture can first be extruded separately and created as composite filaments, and then the desired filament is 3D printed using extrusion printer [95,96].

In general, the amount of polymer used in these methods is higher than in the suspension methods, because the addition of ceramic particles has a strong effect on the formed melt paste, and by increasing a small amount of ceramic powder, the possibility of forming a filament to make parts is increased, and with this increase, the depreciation rate of the extrusion nozzle also increases. The general advantages of these methods include ease of use, insensitivity to changes in the amount of polymer matrix or ceramic particles, the production of parts with different dimensions and the low cost of part manufacturing [95]. On the other hand, when formulating the desired paste composition or subsequently for filament production, the commercialization process can be facilitated and composite films with a specific composition can be supplied wholesale and commercially to manufacturers. Initially, this method was developed only for the 3D printing of polymers, but after the attention of many researchers, the production of composite filaments containing ceramic particles, obtained by breaking the pieces, using a polymer matrix, became possible, as well as high quality composite parts. One of the advantages of these methods is the use of thermoplastics, which are mostly soft materials, on the other hand, the manufacturing parameters of the composition of materials and the characteristics of the ceramic particles used in polymers are factors affecting their mechanical properties [4,97].

5.2.1. Fused deposition modeling

This method is a technique based on fused filament fabrication [98–101] in which a filament containing a large amount of ceramic particles is mixed with quantities of a thermoplastic polymer such as wax and then printed using standard FDM printers [102]. Figure 9 shows the manufacturing process for the filament-extruded product. The employment of FDM facilitates the directed placement of individual, pre-impregnated filament lines, thereby obviating the necessity for costly molds and enabling the fabrication of more intricate components with elevated curvatures [103].

The thermoplastic filament is applied to the nozzle as a rotating pressure roller and is affected by the heat of the melt, causing it to melt and then be applied to the intended platform [104–106]. FDM can be considered as a form of rapid prototyping, and is, in general, comparable to injection molding. In comparison to other manufacturing techniques, FDM is a cost-effective method that can be performed with relatively simple equipment and inexpensive materials [21,107]. Based on recent studies conducted by researchers, composite parts made by robocasting and FDM were evaluated in a series of parameters determined for the quality production of parts, and the result of this evaluation is shown below in Table 4 [13].

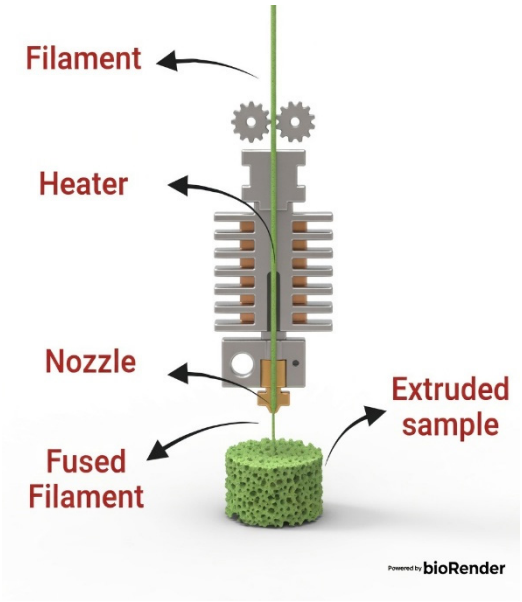

Fig. 9. FDM additive manufacturing method using film.

The filament components necessary for this process include: (1) a base polymer, which serves as the filament's backbone and provides mechanical strength; (2) an elastomer-based polymer to impart elasticity and flexibility; (3) a tackifier to enhance adhesion and flexibility; (4) a plasticizer to provide plasticity for spooling; and (5) wax to reduce the melt viscosity. The resulting filaments are optimized in terms of strength, elasticity, plasticity and flexibility. This process has been employed in the manufacture of a diverse array of oxide and non-oxide ceramics [108]. Nevertheless, the range of applications is constrained by the mechanical and rheological properties that are necessary for the production of different components [101,109]. It is therefore essential to conduct a detailed study of the rheological properties and parameters in order to ensure the correct flow and exit of the molten filament from the nozzle [105,110].

For example, it is possible that the filaments used are not hard enough and break on the way and on entry into the nozzle, which is an indication of the filaments' inability to maintain flow continuity for part production [111, 112]. Screw extrusion has emerged as a highly effective approach for producing dense ceramic parts through FDM. This method provides superior control over the printing process, enhances the reliability of highly-filled ceramic feedstocks, and enables precise regulation of filament rheology compared to conventional single-screw or piston

Table 4. Comparison of robocasting and FDM by main processing parameters.

Performance	Robocasting	FDM
Resolution	High	Medium
Size of parts made	Large	Small
Geometrical complexity	Medium	Medium
Surface roughness	Medium	Medium
Manufacturing process cost	Low	Medium
Powder size	Fine	Fine
Amount of binder in green part	Low	High
State of suspension (paste or slurry)	Paste	Filament

Table 5. Investigated properties of final silicon nitride parts by FDM manufacturing.

AM process	Ceramic material	Ceramic powder loading, vol.%	Shrinkage, %	Density, %		Flexural strength, MPa	Refs.
				Green	Final		
Fused deposition modelling of ceramics	Si_3N_4	55	16.6 ± 1.3 in XY 19.3 ± 1.6 in Z	53	98	824 ± 110 (4-point bending)	[108]
Extrusion free form fabrication	Si_3N_4	53	18 ± 3 in XY 20 ± 5 In Z	51	97	613 ± 12	[74]
Direct ink writing	Si_3N_4	52	16	56	99	737 ± 38	[114]

systems. Because each ceramic suspension possesses distinct rheological characteristics (such as viscosity, yield stress, and shear-thinning behavior), the design of the extrusion screw must be specifically tailored to the feedstock composition. Different extrusion screw configurations have been developed to address these requirements. For example, some designs integrate a combination of a gear wheel and a plunger mechanism, which allows for accurate metering and gentle handling of the material, making them particularly suitable for the production of delicate and high-precision ceramic components. In a prominent study, Scheithauer et al. [16] successfully fabricated dense alumina ceramics reaching a relative density of 99% using an optimized screw extrusion system, demonstrating the capability of this technique to achieve high densification while maintaining good shape fidelity. Table 5 presents a comparison of the manufacture of parts containing silicon nitride with the additive manufacturing processes of robocasting and FDM. In these studies, secondary processes are used to produce the final ceramic parts. It is obvious that the production of composite parts is proposed. Both methods are possible and both methods have produced parts with desirable mechanical properties.

5.2.2. Thermoplastic 3D printing

Thermoplastic 3D printing, which can use a wide range of thermoplastics as a polymer matrix to produce composite parts, has been one of the most popular additive manufacturing methods in recent years. This 3D printing, which can manufacture a variety of polymer composites with metallic and ceramic components, was developed by Scheithauer et al. [16,115] using a combination of robocasting and FDM methods. The process involves casting and dispersing the ceramic powder in a paraffin-based thermoplastic polymer, grinding it at 100 °C and sending it to a heated extrusion press to be applied by a 3D printer, which uses the thermoplastic binder system to create a dense composite [116]. This method also allows the manufacture of metallic parts and enables the adoption of both continuous and droplet deposition strategies for the manufacture of other parts [117] which is shown in Figure 10.

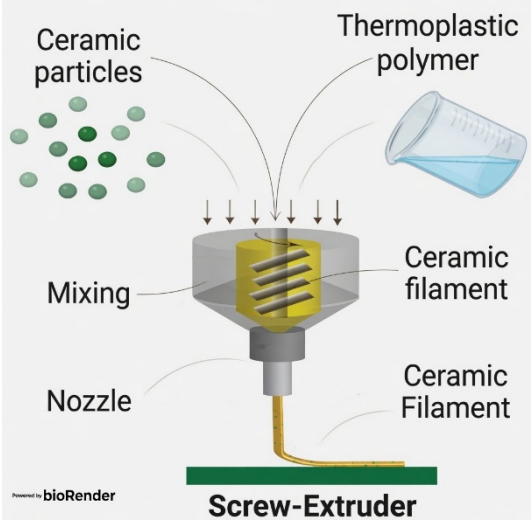

Fig. 10. Schematic of the thermoplastic 3D printing process.

The advantages of using this method are essentially a combination of the advantages of using the two methods mentioned above, with the result that different amounts of additives can be added and different polymers can be used at the same time, in addition to creating complex geometric shapes. In addition, there is no limit to the use of a wide range of materials that are used in the additive manufacturing process. Among the advantages of this method over FDM, it is possible to mention the shortening of part construction and the elimination of the initial mixing and extrusion of materials to create the filament. In addition, the raw materials used can be used directly if they are in short supply and cannot be made into filaments by separate extrusion [118].

6. POST-PROCESSING: DE-BINDING AND SINTERING

Transforming the as-printed green body into a dense, functional ceramic component requires careful post-processing. This involves two critical stages: *de-binding* (removal of the organic binder matrix) and *sintering* (densification of the ceramic particles). These steps significantly influence the final microstructure, density, dimensional accuracy, and mechanical properties of EBAM-produced ceramics.

6.1. De-binding strategies

De-binding is frequently the most time-consuming and defect-prone stage in the EBAM process chain. Incomplete or overly rapid binder removal can lead to cracking, blistering, warping, or residual carbon contamination, which compromises subsequent sintering. Three primary de-binding strategies are commonly employed, often in combination (two-step processes) to optimize efficiency and minimize defects (Figure 11).

Thermal de-binding involves controlled heating of the green body to pyrolyze or evaporate the binder. Typical heating rates are slow (0.1–2 °C/min, often ≤ 1 °C/min in critical decomposition ranges) to allow gaseous by-products to diffuse out without generating excessive internal pressure. Temperatures generally range from 400–600 °C (up to 900–1100 °C in some multi-stage profiles), conducted in air (for oxide ceramics such as Al_2O_3 and ZrO_2), inert atmospheres (argon or nitrogen for non-oxides like SiC or Si_3N_4), or vacuum to reduce oxidation risks. Hold times at key decomposition temperatures (identified via thermogravimetric analysis and differential scanning calorimetry (TGA/DSC)) can extend from several hours to days, depending on part geometry and wall thickness [60].

Solvent de-binding (or solvent extraction) is often used as a first step for multi-component binder systems. The green part is immersed in a suitable solvent (e.g., water or ethanol for polyethylene glycol (PEG), hexane or acetone for waxes/paraffin) at moderate temperatures (typically 40–80 °C). This selectively dissolves the low-molecular-weight primary binder, creating interconnected pore channels that facilitate subsequent thermal removal of the backbone polymer. Solvent de-binding is relatively fast and cost-effective but is limited to smaller cross-sections and requires careful control to avoid cracking from capillary stresses [119].

Catalytic de-binding, primarily applied to polyoxymethylene (POM)-based binder systems, offers the fastest removal. The process exposes the green body to an acidic vapor atmosphere (commonly nitric acid, HNO_3) at relatively low temperatures (110–140 °C, sometimes up to 120–150 °C). This catalyzes the depolymerization

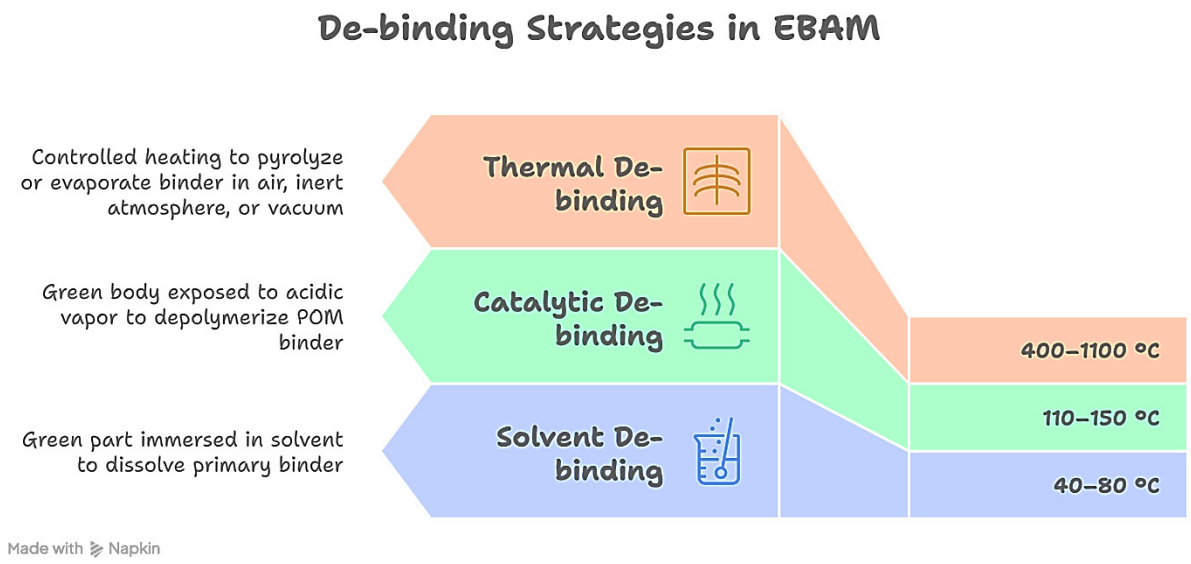

Fig. 11. De-binding strategies in EBAM.

of POM into formaldehyde gas, which diffuses rapidly out of the part. De-binding times can be reduced from days (thermal) to hours, with minimal dimensional distortion and low carbon residue. This method is particularly advantageous for thicker sections (> 30 mm in some feedstocks) and is well-adapted from ceramic injection molding (CIM) experience [120].

Hybrid approaches (e.g., solvent + thermal or catalytic + thermal) are widely recommended to balance speed, safety, and defect minimization. A number of investigations have indicated emphasize the importance of TGA/DSC for designing multi-stage profiles with optimized hold times and atmospheres to prevent defects.

6.2. Sintering methods and shrinkage anisotropy

After de-binding, the resulting brown body undergoes sintering to achieve densification through particle rearrangement, neck formation, and pore elimination. Conventional pressure-less sintering in air or controlled atmospheres remains the standard for most EBAM ceramics, typically at 1200–2000 °C depending on the material (e.g., ~ 1550–1650 °C for Al_2O_3, higher for SiC or ZrO_2). Heating rates during sintering are usually 1–5 °C/min, withhold times of 1–5 hours to reach > 95–99% theoretical density.

To address limitations of conventional sintering—such as prolonged processing times and excessive grain growth—advanced sintering techniques are increasingly applied to EBAM-produced ceramic parts. These include:

- Microwave sintering. Petit et al. [121] demonstrated that microwave sintering offers volumetric heating, which enables significantly faster densification rates and reduced grain growth. This technique has been successfully combined with material extrusion additive manufacturing, particularly in the sintering of 3Y-TZP zirconia parts.
- Spark plasma sintering (SPS). Brucculeri et al. [122] showed that spark plasma sintering provides rapid consolidation under simultaneous uniaxial pressure and pulsed electric field, allowing short sintering times while achieving high density. This method has been effectively applied for post-processing of complex structures produced by material extrusion.
- Hot pressing and flash sintering. Nunes et al. [123] reported that hot pressing and flash sintering enable ultra-fast densification with minimal thermal exposure. In particular, flash sintering has shown excellent potential for the rapid consolidation of 3D-printed ceramic scaffolds with reduced energy consumption.

These advanced techniques help retain fine microstructures, suppress excessive grain growth, and improve the mechanical properties of the final EBAM components.

A major challenge unique to EBAM (and other extrusion-based methods like FFF and robocasting/DIW) is *shrinkage anisotropy*. The layer-by-layer deposition and shear-induced particle/filament orientation during extrusion create microstructural anisotropy, including preferential pore alignment and inter-filament interfaces. Consequently, linear shrinkage in the build direction (Z-axis) is typically higher than in the printing plane (X-Y directions). Reported differences range from 2–5% or more (e.g., ~ 17% in X-Y vs. ~ 21% in Z for some alumina FFF parts), leading to distortion, warping, or internal stresses if not compensated [124,125].

This anisotropy arises from the filament deposition process and is more pronounced in filament-based systems than in direct ink writing. Mitigation strategies include anisotropic scaling in CAD design (different compensation factors for X-Y and Z), optimized printing parameters (e.g., infill patterns, raster orientation), and controlled sintering profiles. Predictive modeling of anisotropic sintering behavior is an emerging tool for improving dimensional accuracy [126].

Overall, successful post-processing in EBAM requires integrated optimization of de-binding and sintering parameters tailored to the specific binder system, ceramic powder, and part geometry. Advances in multi-step de-binding and rapid sintering techniques continue to reduce processing times and defects, enhancing the viability of EBAM for producing complex, high-performance ceramic components (Table 6).

7. PARAMETERS AFFECTING EXTRUSION-BASED 3D PRINTING

In the 3D extrusion-based printing of polymer composites, a broad spectrum of processing parameters can be identified, each contributing in a unique way to the print quality, microstructural evolution, and overall performance of the fabricated components. These parameters influence not only the deposition behavior and interlayer bonding, but also the mechanical integrity and functional characteristics of the final structure. For the sake of clarity and systematic analysis, these numerous parameters can be broadly classified into two principal categories, which will be comprehensively described and examined in the following sections: (1) parameters affecting the paste and (2) 3D printing machine parameters. These categories are illustrated in Figure 12. Parameters affecting the paste refer to the intrinsic characteristics of the feedstock, such as particle size, particle size distribution, solid loading, binder type, and additives, which directly govern the rheological behavior, printability, and quality of the extruded material. In contrast, 3D printing machine parameters include operational variables such as layer height, print speed, extrusion temperature, and nozzle diameter, which influence the deposition process, interlayer bonding, and overall structural integrity of the printed part. While paste-related parameters primarily determine the material's extrudabil-

Table 6. Sintering parameters and properties of EBAM ceramics.

Ceramic system	Sintering method	Temperature range, °C / atmosphere	Final density, %	Flexural strength, MPa	Shrinkage (X.Y–Z), %
Al_2O_3	Conventional pressureless	1550–1650 / air	97–99	300–450	15.2–18.1
ZrO_2 (3Y-TZP)	Microwave-assisted or conventional	1400–1550 / air	98–99.5	500–750	18.5–21.0
Si_3N_4	Hot pressing	1700–1800 / N_2	98–99.5	650–850	16.6–19.3
SiC	Spark plasma sintering (SPS)	1800–1950 / argon	97–99	350–500	14.0–16.5
Hydroxyapatite (HA) – scaffold	Conventional pressureless	1100–1300 / air	90–96 (porous scaffold)	10–50 (compressive)	12.1–14.2

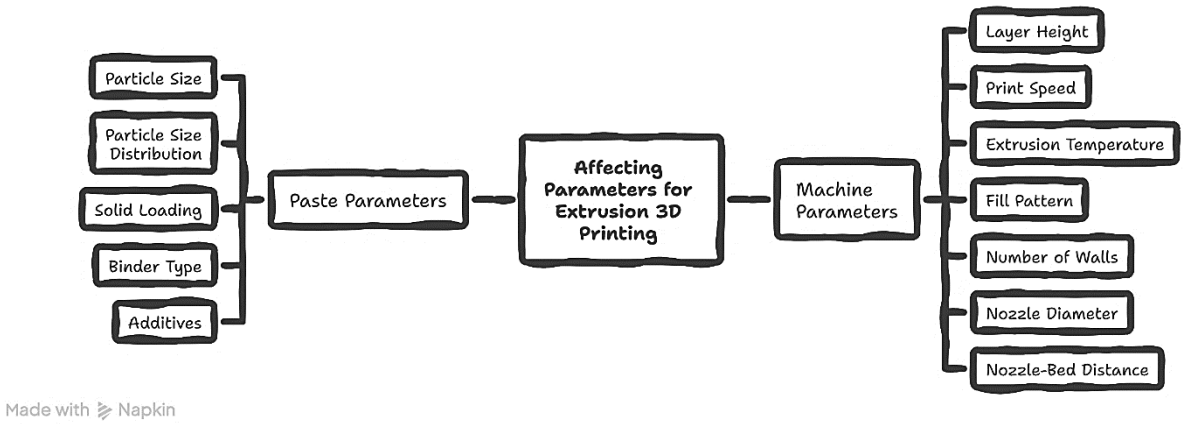

Fig. 12. Affecting parameters for extrusion 3D printing.

ity and stability, machine parameters control the precision and consistency of the layer-by-layer fabrication.

7.1. Parameters affecting the paste

The parameters of the paste are of critical importance, as they significantly influence the printability, quality, and final performance of parts produced by composite paste extrusion printing. These parameters are listed below.

7.1.1. Particle size

The viscosity of ceramic reinforcement particles (< 10 μm) is generally increased, which requires greater pressure to be applied by extrusion. While this increases the phase integrity of the paste, bigger particles (> 10 μm) have the opposite effect. A reduction in paste viscosity may occur, accompanied by an increased likelihood of nozzle clogging. Furthermore, the phase integrity of the paste may also be compromised [127]. The particle size and distribution also exert a direct influence on the density of the final product [128].

7.1.2. Particle size distribution

This parameter is also effective in the viscosity of composite pastes. The more uniform the size distribution of ceramic particles is, the more suitable it is for the desired application. However, if this distribution has a wide range, the viscosity increases [127].

7.1.3. Solid loading

The loading of solid particles is typically conducted at loads exceeding 50 vol.%, which has been observed to result in an increase in viscosity and yield stress. Additionally, the formation of a more robust filament structure has been reported. However, it is important to note that this loading approach also leads to an increase in the required pressure for extrusion. A reduction in the loading of solid particles to less than 50 vol.% has been observed to result in a decline in both the viscosity of the composite paste and the strength of the filament formed from the paste. Consequently, the optimal loading amount for each ceramic material should be identified [127].

7.1.4. Binder type

The selection of an appropriate polymer binder is critical, as it directly governs the rheological properties of the paste, including viscosity, shear-thinning behavior, and yield stress. A well-chosen binder enhances particle dispersion and interfacial adhesion within the polymer matrix, enabling the preparation of homogeneous, high-quality composite pastes. Consequently, this leads to improved printability and superior mechanical properties in the final printed components [128].

7.1.5. Additives

The selection of appropriate additives can result in a reduction in the amount of solvent required for the process of manufacturing the part. Additionally, these additives exert a significant influence on the rheology of pastes, with the most crucial role of modifying doughs pertaining to this category of materials [128].

7.2. 3D printing machine parameters

The aforementioned parameters have a considerable impact on the mechanical properties of the produced parts, which are as follows.

7.2.1. The height of the formed layers

Reducing the layer height generally improves the mechanical properties of the printed part by minimizing the size of interlayer defects and enhancing interlayer bonding [129]. However, this relationship is not unlimited. When the layer thickness approaches or becomes comparable to the size of the ceramic particles, printability deteriorates and new defects such as nozzle clogging, poor particle packing, and increased porosity may occur. Moreover, the optimal layer height depends not only on particle size distribution but also on the part topology and geometric complexity. Therefore, layer height must be carefully optimized according to the specific feedstock characteristics and the intended application to achieve the best compromise between mechanical performance and printing reliability.

7.2.2. Print speed

Print speed is a critical process parameter that significantly influences the quality and mechanical performance of extrusion-based printed parts. An optimal printing speed must be determined for each specific material and geometry. If the printing speed is excessively high, the interlayer cooling time decreases substantially, leading to insufficient diffusive bonding and poor interfacial adhesion between consecutive layers, which ultimately reduces the overall mechanical strength of the component. Conversely, excessively low printing speeds can cause material degradation, over-heating, or excessive spreading of the extruded filament.

Importantly, the effect of print speed on mechanical properties is highly dependent on part geometry and the resulting molecular or particle orientation. In certain orientations and geometries, an appropriately selected printing speed can enhance molecular alignment and interlayer diffusion, thereby improving the anisotropic mechanical strength of the printed part [130].

7.2.3. Extrusion temperature

In all extrusion printing methods, the application of heat has a significant effect on the properties and quality of the part. This is true even in methods in which the heat applied to the part is not defined. In such cases, the role of temperature changes is nevertheless important [131]. For example, at a relatively high optimized extrusion temperature, an improvement in the link between the layers is observed.

7.2.4. Fill pattern

The fill pattern, also known as the infill pattern, plays a critical role in determining the density, mechanical strength, and overall performance of the printed part. Different infill geometries directly influence the internal structure and load-bearing capacity of the component. In particular, studies have shown that grid patterns can significantly improve part density and mechanical properties compared to other infill designs [132].

7.2.5. The number of walls

Increasing the number of walls (perimeters) has been shown to improve the overall quality of the printed components. A higher number of walls enhances surface finish, structural rigidity, and mechanical strength by providing additional solid outer layers around the infill [109].

7.2.6. Nozzle diameter

The nozzle diameter is a key process parameter that must be properly matched with the rheological properties (especially viscosity and yield stress) of the composite paste. An incompatible nozzle diameter—typically too small for a highly viscous paste—can cause excessive pressure buildup, nozzle clogging, irregular extrusion, or even damage to the printed part, ultimately compromising its mechanical strength. Conversely, when the nozzle diameter is appropriately selected, it enables stable and uniform filament extrusion, resulting in defect-free parts with

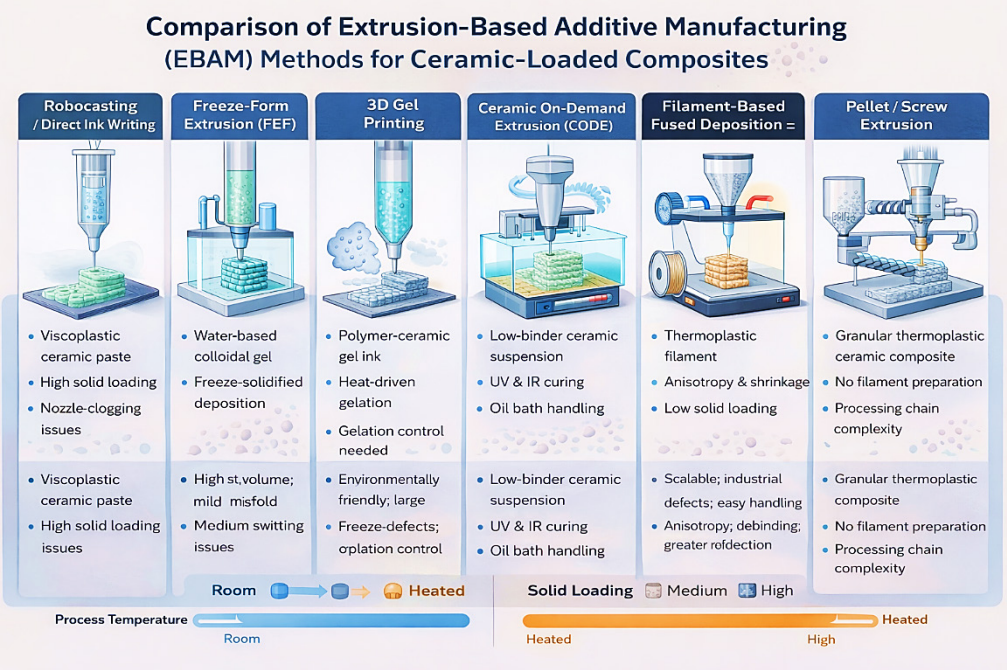

Fig. 13. Comparison of EBAM manufacturing processes.

consistent geometry and improved mechanical performance [130,109].

7.2.7. The distance between the nozzle tip and the bed

The distance between the nozzle tip and the build bed (also referred to as gap height or layer height) is a critical printing parameter. It should be carefully adjusted so that the extruded filament diameter is slightly larger than the nozzle-to-bed distance. This slight over-extrusion ensures proper layer compression, resulting in excellent interlayer adhesion, dense structures, and defect-free layers with smooth surfaces [130,109].

Ultimately, the optimal mode of each parameter affecting the paste required for composite part production, as well as the parameters affecting additive extrusion printing equipment, must be determined. This includes the crucial activities of every researcher involved in the production of composite parts using 3D printers. By paying close attention to this issue, an extrusion process can be developed that produces parts with exceptional capabilities in the desired application conditions.

8. COMPARATIVE SUMMARY OF EBAM TECHNIQUES

EBAM encompasses a family of processes that deposit highly loaded ceramic-polymer feedstocks layer-by-layer, enabling the production of complex polymer-ceramic composites or near-net-shape dense ceramics after de-binding and sintering. The choice of technique critically influences achievable ceramic loading, shape fidelity, final density, mechanical performance, scalability, and post-processing demands. Suspension-paste methods (e.g., robocasting/DIW, FEF, 3D gel printing, and CODE) generally permit higher ceramic contents (> 50 vol.%) and room-temperature operation, while thermoplastic/filament-based approaches (FDM and thermoplastic 3D printing) offer greater process stability and commercial feedstock availability but introduce additional thermal and rheological constraints. Over the past decade, comprehensive reviews highlight that no single technique dominates universally; instead, selection depends on target application requirements such as resolution, part size, density, or multi-material capability (Table 7). A comprehensive comparative analysis of the binder systems, synthesized from both the existing literature and recent peer-reviewed studies, is presented in Figure 13.

8.1. Analytical discussion

Suspension-paste techniques consistently outperform filament-based methods in ceramic loading and green-body density because the liquid carrier (water or solvent) enables higher solids fractions without compromising extrudability, provided yield-pseudoplastic rheology is achieved (yield stress 100–1000 Pa, shear-thinning behavior). DIW/robocasting, in particular, excels for highly loaded pastes (> 55 vol.%) and allows in-situ alignment of high-aspect-ratio reinforcements (e.g., carbon fibers in SiC composites), yielding fracture-toughened structures with non-catastrophic failure modes [52]. However, these

Table 7. Comparative summary of major EBAM techniques for highly-filled polymer-ceramic composites and dense ceramics manufacturing.

Technique	Feedstock type	Max ceramic loading, vol.%	Resolution (nozzle), μm	Resolution (layer), mm	Typical sintered density, %	Achievable flexural strength, MPa	Key advantages	Main limitations	Representative applications	Ref.
Robocasting / DIW	Aqueous or solvent-based viscoplastic suspension	40–60	200–800	0.3–0.5	96–99	Al_2O_3: 150–350; Si_3N_4: up to 350	High solid loading; excellent shape retention; no support needed	Rheology sensitivity; drying cracks; nozzle clogging	Porous scaffolds, CMCs, aerospace structures	[39]
Freeze-form extrusion (FEF)	Water-based colloidal gel	50–65	400–800	0.4–0.8	97–98	50–300 (porosity-dependent)	Environmentally friendly; large parts; low binder	Freeze defects; dimensional instability	FGMs, structural ceramics	[83]
3D gel printing	Polymer-ceramic gel (in-situ crosslinking)	50–60	300–600	0.3–0.6	95–98	100–400 (material-dependent)	Large-scale capability; low cost; tunable systems	Gelation control; shrinkage; limited resolution	Complex thermoset composites	[133]
Ceramic on demand extrusion (CODE)	Low-binder suspension + oil bath + IR curing	50–65	200–500	0.2–0.5	98–99.5	UHTCs (e.g., ZrB_2): high (> 400)	Near-full density; minimal cracking; multi-material	Process complexity; low throughput	UHTCs, sensors, heat exchangers	[75]
FDM (filament-based)	Ceramic-filled thermoplastic filament	40–55 (effective < 50)	400–600	0.1–0.3	90–92	Si_3N_4: up to 800; ZrO_2: ~ 400; Al_2O_3: 200–300	Scalable; industrial maturity; easy handling	Anisotropy; de-binding defects; shrinkage (15–30%)	Biomedical parts, structural ceramics	[134]
Pellet/screw extrusion	Granular thermoplastic–ceramic composite	45–60	400–1000	0.2–0.8	97–99	Comparable or slightly higher than FDM	No filament prep; better homogeneity; scalable	Screw design complexity; resolution limits	Dense ceramics, hybrid systems	[117]

processes are sensitive to drying kinetics; uncontrolled evaporation induces capillary stresses, cracking, and warping—issues mitigated in FEF by controlled freezing and lyophilization or in CODE by continuous oil-bath immersion and infrared curing, which achieve near-theoretical densities (> 99%) with minimal residual porosity.

In contrast, thermoplastic/filament-based EBAM (FDM and direct pellet extrusion) benefits from the mechanical integrity of pre-compounded filaments or granules, enabling commercial-scale production and support-structure generation for overhangs. Recent filament formulations reach 60 vol.% loading with optimized multi-component binders (primary + backbone + additives), and ultrafast or microwave sintering now routinely delivers > 98% density with flexural strengths rivaling or exceeding conventional ceramics. Nevertheless, these methods suffer from pronounced anisotropy (Z-direction weakness due to interlayer bonding) and larger shrinkage (up to 28% in Z), necessitating precise oversizing and sophisticated de-binding protocols (thermal, catalytic, or solvent-assisted) to avoid cracking or blistering.

Post-processing and densification trade-offs are decisive. Suspension routes typically require simpler solvent removal but risk delamination during drying, while filament routes demand energy-intensive multi-stage de-binding yet benefit from modern innovations such as ultrafast high-temperature sintering (UHS) that achieve crack-free 99% density in seconds [106]. CODE uniquely bridges both worlds by combining low-binder suspensions with controlled layer-wise drying and partial sintering via infrared, making it ideal for ultra-high-temperature ceramics (UHTCs) and functionally graded materials (FGMs).

Mechanical performance follows loading and defect density: DIW and CODE routinely produce parts with flexural strengths > 300 MPa and Weibull moduli > 10 when optimized, while FDM excels in Si_3N_4 (up to 824 MPa) thanks to tailored deposition paths (contour offset). Anisotropy remains the universal challenge across all EBAM variants; recent multi-nozzle and dynamic-mixing systems enable true multi-material and graded structures, partially alleviating property gradients.

Scalability, cost, and sustainability further differentiate the techniques. Paste-based methods (DIW, 3D gel printing) offer the lowest equipment cost and largest build volumes (up to meter-scale), making them attractive for biomedical scaffolds and large structural components. Filament-based routes leverage existing polymer-printer infrastructure, lowering entry barriers but increasing feedstock cost and waste during de-binding. Environmentally, FEF and aqueous CODE minimize organic content, aligning with circular-economy goals.

New advancements include machine-learning-guided rheology optimization, closed-loop sensor control for filament geometry, hybrid sol–gel/UV-curable inks, and eco-friendly binders, pushing EBAM toward industrial viability for aerospace (UHTCs), biomedical (patient-specific implants), and energy (heat exchangers, sensors) sectors. Multi-material EBAM, particularly CODE and thermoplastic variants, now routinely fabricates FGMs with programmable thermal/electrical gradients.

In summary, DIW/robocasting remains the workhorse for research-scale high-loading complex parts, CODE for highest-density functional ceramics, and filament-based methods for rapid prototyping and commercial scalability. Selection should be guided by required ceramic loading, part size, tolerance to post-processing shrinkage, and target mechanical isotropy. Hybrid approaches—combining DIW with thermoplastic extrusion or integrating in-situ monitoring—represent the most promising pathway toward defect-free, high-performance ceramic components that outperform traditional forming routes in complexity and customization. Future integration of four-dimensional (4D) printing, recyclable binders, and artificial intelligence (AI)-driven process design is expected to further expand the capabilities and industrial adoption of EBAM in advanced ceramic manufacturing [135].

8.2 Critical evaluation of conflicting literature and recent advances

This section provides a critical evaluation of recent developments in the field, with particular emphasis on the relationships between processing conditions, microstructural evolution, and resulting material properties. Special attention is given to reported inconsistencies and divergent trends across different studies, which often arise from variations in feedstock formulation, processing parameters, and characterization methodologies. The aim is to reconcile these discrepancies and highlight coherent trends that can guide future optimization strategies.

While EBAM has demonstrated substantial progress in processing highly-filled polymer-ceramic feedstocks, a critical examination of the literature reveals several areas of conflicting findings and unresolved challenges that warrant deeper scrutiny. For instance, studies on ceramic loading consistently highlight the trade-off between rheological printability and final densification [39]. Some authors report successful extrusion at solid loadings exceeding 60 vol.% in aqueous suspensions for DIW/robocasting, achieving post-sintering densities > 98% with minimal defects. However, others note pronounced limitations in filament-based FDM/FFF systems, where loadings above 50–55 vol.% often lead to nozzle clogging, filament brittleness, and significant anisotropic shrinkage (up to 15–30% in the Z-direction), resulting in warping and reduced interlayer bonding [136–138].

This discrepancy arises primarily from differences in binder systems and extrusion mechanisms. Aqueous or

gel-based suspensions (e.g., CMC/HPMC or Pluronic) enable higher loadings and better shape retention due to yield-pseudoplastic behavior but are more susceptible to drying-induced cracking and capillary stresses. In contrast, thermoplastic filaments offer superior handling and compatibility with commercial printers but suffer from higher organic content, complicating de-binding and increasing the risk of carbon residue or blistering. Recent meta-analyses confirm that while DIW excels in complex porous scaffolds, FDM provides better scalability for dense structural parts—yet direct quantitative comparisons remain scarce due to variations in powder characteristics (size, morphology) and sintering protocols [139].

Recent publications from 2025–2026 further illuminate these tensions and propose mitigation strategies. González-Suárez et al. [136] emphasize sustainability challenges in material extrusion of ceramics (MEX-AM), noting that while low-binder aqueous systems reduce environmental impact, they often compromise green-body strength compared to thermoplastic routes. Wang et al. [138] introduce a defect-driven framework for hybrid extrusion processes, addressing geometric inaccuracy, porosity, and weak interlayer bonding through multiscale optimization—highlighting that uncontrolled defects in conventional EBAM can reduce mechanical reliability by 20–40% [136–138].

In polymer-derived ceramics (PDCs), Khuje et al. [140] and Bishop et al. [141] demonstrate that filler strategies (e.g., SiC or carbon reinforcements) effectively mitigate shrinkage and cracking in DIW of preceramic polymers, achieving near-net-shape UHTCs with improved fracture toughness. However, conflicting results persist regarding multi-material integration: while some studies report successful co-extrusion of graded structures (e.g., ZrB_2–SiC), others highlight interfacial delamination during co-sintering due to mismatched shrinkage and thermal expansion [140,141].

These recent works underscore the need for integrated process–structure–property modeling and standardized testing protocols. Future research should prioritize hybrid approaches (e.g., DIW combined with in-situ IR curing or microwave-assisted sintering) and AI-optimized rheology to resolve these conflicts, bridging the gap between laboratory-scale demonstrations and industrial scalability. By addressing these limitations, EBAM can more effectively transition from prototyping to reliable production of high-performance ceramic components [142].

9. APPLICATIONS

The geometric flexibility and material versatility inherent to EBAM—encompassing filament-based fused deposition modeling (FDM/FFF), direct ink writing (DIW), robocasting, and related paste- or slurry-extrusion techniques—when combined with highly filled polymer-ceramic feedstocks (typically 50–85 vol.% ceramic loading), have enabled an exceptionally broad spectrum of advanced applications. These span biomedical, aerospace and defense, electronics and sensor systems, energy conversion/storage, and structural/high-temperature engineering domains. Unlike conventional ceramic processing routes (e.g., slip casting, injection molding, or subtractive machining), EBAM uniquely facilitates the layer-by-layer deposition of complex, patient- or application-specific architectures with controlled microstructural features—such as graded porosity, internal lattices, conformal channels, and multi-material integrations—at multiple length scales. This capability optimizes functional performance (mechanical, thermal, electrical, and biological) while minimizing material waste and tooling costs, positioning EBAM as a transformative technology for next-generation components. Recent advancements (up to 2025–2026) in feedstock rheology, multi-material co-extrusion, and post-processing (de‑binding/sintering) have further elevated achievable densities (> 95–99% theoretical), mechanical strengths, and functional properties, often rivaling or surpassing traditionally manufactured counterparts [143–148].

9.1. Biomedical applications

EBAM has become a cornerstone for fabricating patient-specific biomedical implants, tissue-engineering scaffolds, and dental restorations, leveraging biocompatible ceramics such as hydroxyapatite (HA), β-tricalcium phosphate (β-TCP), biphasic calcium phosphates (BCP), and zirconia (ZrO_2 or 3Y-TZP). In bone regeneration, DIW/robocasting of HA- and TCP-based inks produces highly controlled macroporous architectures with pore sizes optimally tuned to 300–600 μm (and interconnected microporosity < 10 μm), promoting osteoconduction, vascularization, and nutrient diffusion. Compressive strengths routinely reach 50–150 MPa (and up to higher values with polymer infiltration or optimized sintering), closely mimicking trabecular bone while enabling graded porosity designs—dense outer shells transitioning to highly porous cores—for enhanced biological integration and mechanical reliability under load-bearing conditions. Recent studies demonstrate in vivo bone regeneration efficacy, with scaffolds supporting mesenchymal stem cell differentiation, mineralization, and defect healing in animal models; drug-loading (e.g., vancomycin or growth factors) via multi-material extrusion further enables localized antimicrobial or osteogenic delivery without compromising printability [143]. Representative examples of such high-precision extrusion-based printing are shown in Figure 14, which presents SEM micrographs and optical images of 21-layer segmented poly(ester urethanes)/poly(3-hydrox-

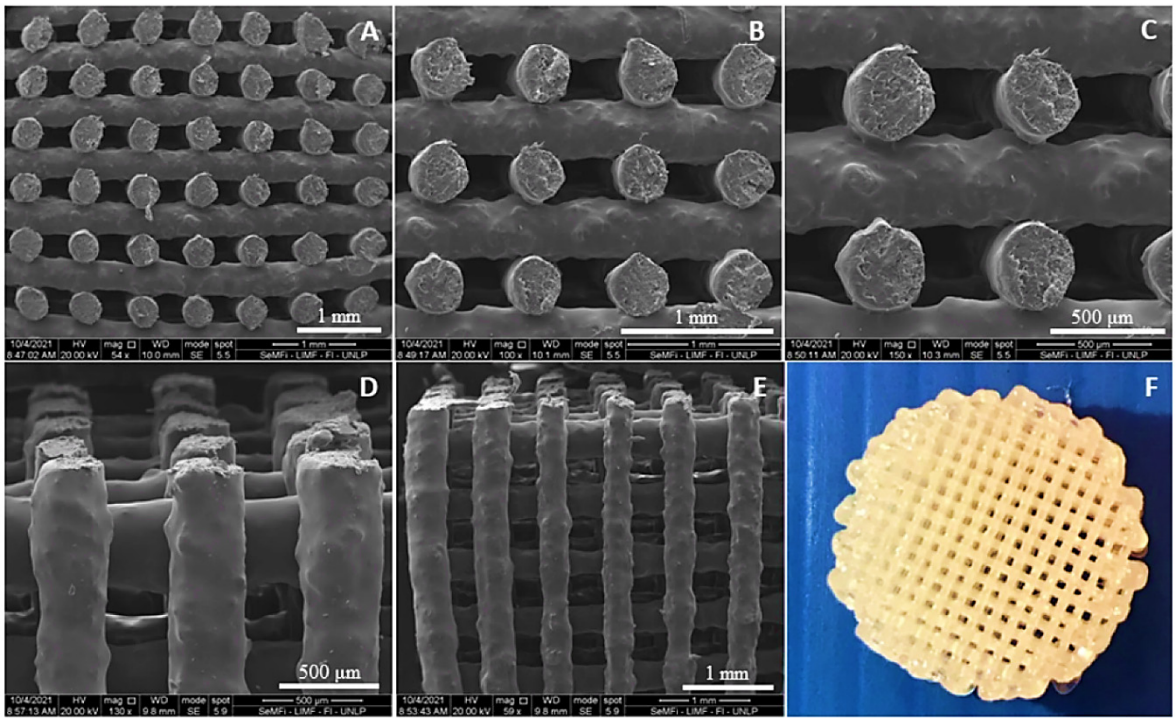

Fig. 14. Printed structures of SPEU-PHBV (21 layers bio-glass scaffolds for tissue engineering). SEM micrographs: (A–C) cross-sectional view (55×, 100×, and 150×), (D,E) top view (130×, 60×), and (F) image of the 3D-printed structure (top view, 15 mm diameter). Reproduced from Ref. [144] under the terms of CC BY 4.0 license. © 2024 Lores et al.

ybutyrate-co-3-hydroxyvalerate) (SPEU-PHBV) structures fabricated via DIW. These images highlight the excellent filament uniformity, layer adhesion, and overall architectural control achievable with polymer-based inks, demonstrating the technique's suitability for producing complex biomedical scaffolds [144].

In dental applications, extrusion-based processes (including FDM with highly filled zirconia filaments or gelled suspensions) have been successfully applied to fabricate 3Y-TZP or 5Y-PSZ crowns, bridges, implants, and abutments. These exhibit marginal fit accuracies below 50 µm (clinically acceptable), full densification (> 99% relative density), flexural strengths exceeding 1000 MPa, hardness ~ 15–16 GPa, and translucency comparable to milled zirconia—satisfying ISO 6872 standards for permanent restorations. Patient-specific geometries derived from cone beam computed tomography (CBCT) or intraoral scans allow customization of occlusal surfaces, root analogs, and overdenture bars (including lattice designs for weight reduction).

Bioactive surface functionalization and multi-phase integration (e.g., zirconia with glass-ceramics) enhances osseointegration, wear resistance in chewing simulators, and long-term stability. Compared to subtractive CAD/CAM milling, EBAM reduces material waste, enables same-day chairside production (via rapid de-binding/sintering protocols), and supports complex internal features impossible with traditional methods. Challenges such as anisotropic shrinkage (~ 15–20% linear) are mitigated through CAD compensation and optimized raster patterns, yielding reliable clinical outcomes [145].

9.2. Aerospace and defense applications

For extreme-environment applications, EBAM excels in producing ultra-high-temperature ceramics (UHTCs) such as zirconium diboride (ZrB_2), ZrB_2–SiC composites, and zirconium carbide (ZrC), critical for thermal protection systems (TPS), engine nacelles and turbine ducts, hypersonic vehicle leading edges, rocket nozzles, and nuclear thermal propulsion components. These materials maintain structural integrity, oxidation resistance, and mechanical strength at temperatures > 2000–3000 °C, far surpassing metals or conventional ceramics. Extrusion processes (e.g., CODE or filament-based material extrusion additive manufacturing (FMEAM)) enable near-net-shape fabrication of complex internal geometries—conformal cooling channels, lattice reinforcements, and triply periodic minimal surface (TPMS) structures—that optimize thermal management, reduce thermal stresses, and enhance heat dissipation under hypersonic or plasma exposure. Recent innovations include carbon-fiber-reinforced ZrB_2 inks (up to 11 vol.%), yielding improved fracture toughness, thermal shock resistance, and oxidation behavior post-sintering, with densities > 92–96% theoretical and isotropic shrinkage control [146]. Figure 15 presents a

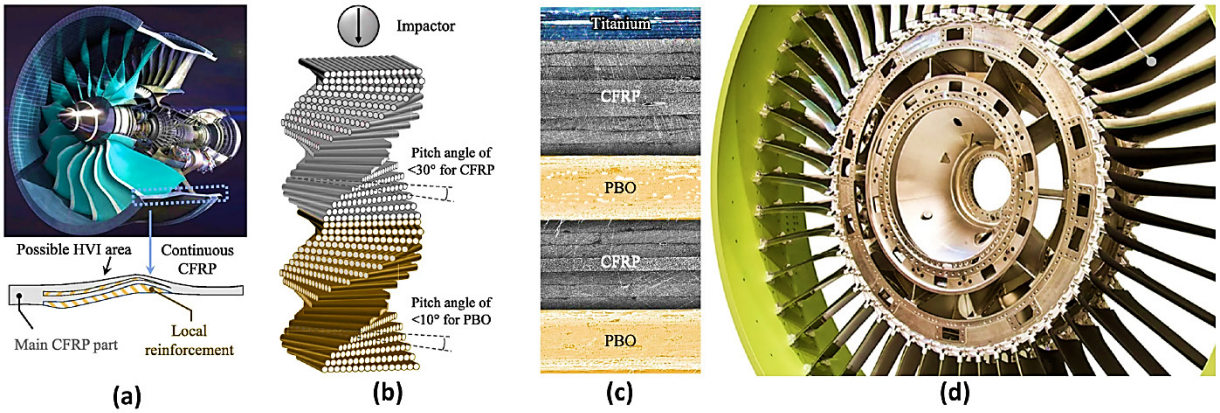

Fig. 15. (a) A cut of an aircraft engine showing its containment casing cross-section and the corresponding schematic at the bottom, (b) bio-inspired helicoidal layup using EBAM 3D printing and (c) hybrid interleaved designs, (d) composite fan case demonstrator developed by GKN Aerospace Sweden. Reproduced from Ref. [147] under the terms of CC BY 4.0 license. © 2025 Shen et al.

cross-sectional schematic of an aircraft engine, illustrating a bio-inspired helicoidal layup design and hybrid interleaved design, along with a turbine engine blade fabricated from carbon fiber-reinforced polymer (CFRP) material made by EBAM 3D printing [147].

Functionally graded materials (FGMs) fabricated via multi-material co-extrusion mitigate thermal expansion mismatches between layers or substrates, enhancing durability in aerospace components. Examples include ZrB_2-based heat exchangers or nuclear fuel elements with tailored porosity for fission gas release. Advantages over subtractive or hot-pressing routes include design freedom for lightweight, hollow structures and scalability for small-batch production without molds. Post-processing (de-binding at low temperatures followed by pressureless or reactive sintering) achieves near-full density while preserving intricate features, making EBAM ideal for next-generation hypersonic vehicles, reusable spacecraft, and high-temperature propulsion systems.

9.3. Electronics and sensor applications

EBAM's ability to process dielectric, piezoelectric, and low-temperature co-fired ceramics (LTCC) has unlocked compact, three-dimensional electronic packaging with integrated functionalities for high-frequency, miniaturized devices. Dielectric ceramics and LTCC feedstocks enable multilayer substrates with embedded conductors, vias, and cavities for RF/microwave components, offering thermal stability up to 400 °C, low coefficient of thermal expansion (~ 4–6 ppm/°C, silicon-matched), and high reliability in aerospace/military electronics. Piezoelectric materials such as barium titanate ($BaTiO_3$), lead zirconate titanate (PZT), or doped variants are extruded into complex lattice or architected structures via filament (60–80 wt.% loading) or robocasting techniques, achieving enhanced electromechanical coupling coefficients through increased surface area, tailored stress distribution, and textured microstructures. Sintered densities > 95%, piezoelectric coefficients (d_{33} ~ 148 pC/N or higher), and dielectric constants > 2000 have been reported, outperforming cast counterparts in sensors, actuators, energy harvesters, and transducers [148].

Multi-material EBAM integrates conductive, dielectric, and piezoelectric phases in a single process—e.g., PZT-PVDF/BNNTs (lead zirconate titanate-polyvinylidene fluoride/boron nitride nanotubes) composites or $BaTiO_3$ with polymer binders—facilitating embedded systems, conformal electronics, and 3D interconnects. Figure 16 shows successful LCD-based UV 3D printing of the developed polymer and BNNT-nanocomposite resins, confirming excellent compatibility for high-resolution macro- and micro-structures. The printed eagle symbol (Fig. 16a) demonstrates outstanding shape fidelity and fine detail (e.g., beak and claws). Initial surface roughness from powder-based resin was easily resolved by quick DI water rinse and air drying. SEM images of micro-scale lattice scaffolds (200 µm struts, 1 mm thick, 50 µm layers) reveal well-defined, tightly stacked layers in both materials (Fig. 16b,c) [149].

Surface roughness was slightly higher for the nanocomposite (10.54 ± 0.68 µm) than the neat polymer (7.68 ± 0.60 µm) due to BNNTs, which also increased flexibility. These results validate the resins for scalable, high-resolution UV additive manufacturing of robust nanocomposite sensors [149]. Recent filament-based workflows confirm rheological optimization for defect-free printing and reliable poling, enabling rapid prototyping of functional electroceramics. These capabilities address demands in 5G/6G communications, IoT sensors, and wearable devices, where geometric complexity enhances performance beyond planar LTCC laminates.

9.4. Energy and structural applications

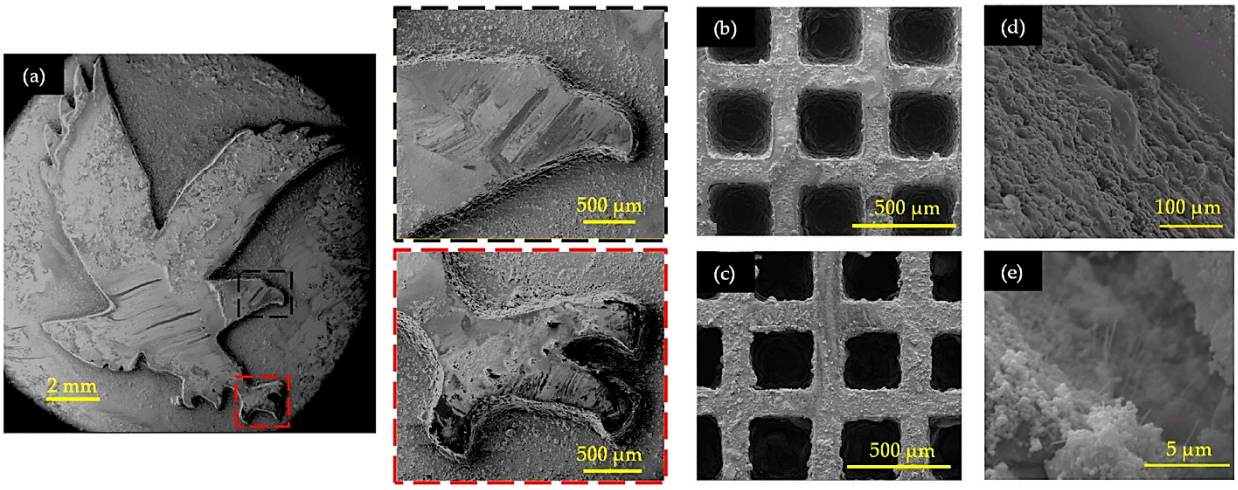

Fig. 16. Printability of developed resins at micro-scale levels: (a) eagle structure with zoomed-in images of beak and claws, lattice structures with 200 µm width printed using (b) 35 wt.% PVDF polymer resin and (c) PVDF/BNNTs nanocomposite resin, (d) zoomed-in layer-by-layer printed nanocomposite structure, and (e) zoomed-in picture of BNNT nanofillers. Reproduced from Ref. [149] under the terms of CC BY 4.0 license. © 2024 Govindarajan et al.

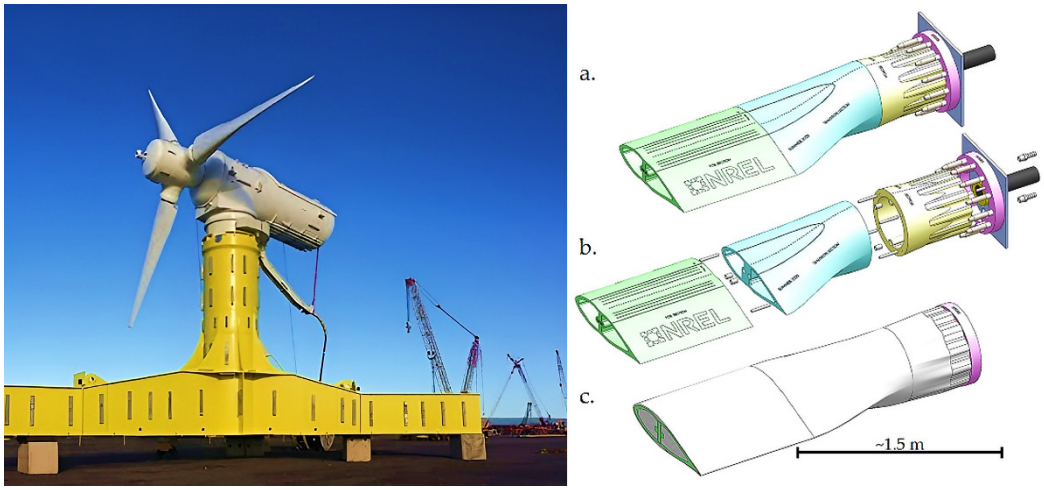

Fig. 17. (Left) A horizontal-axis tidal turbine AR1500® in north-east Scotland (manufactured using EBAM) [152]. (Right) Conceptual 3D design of tidal blade section mold for marine energy system where (a) is fully assembled, (b) is exploded to show the connections between sections, and (c) includes the composite overlay [153]. Adapted from Refs. [152,153] under the terms of CC BY 4.0 license. © 2021 Palmer et al., © 2021 Murdy et al.

In the energy sector, EBAM fabricates key components for solid oxide fuel cells (SOFCs) and electrolyzes, particularly yttria-stabilized zirconia (YSZ, 3YSZ or 8YSZ) electrolytes. FFF/extrusion or robocasting yields thin, high-density (> 95–99%) self-supported or electrolyte-supported structures with micro-patterned or porous surfaces that dramatically increase triple-phase boundary area, boosting ionic conductivity (~ 0.05–0.1 S/cm at 1000 °C—comparable to conventional) and electrochemical performance. Precise layer-thickness control and graded microstructures optimize efficiency while enabling monolithic or reversible solid oxide cells (SOCs) with complex geometries for higher volumetric power density [150].

Beyond electrochemistry, EBAM produces high-performance ceramic heat exchangers using MAX phases—a class of nano-laminated ternary carbides and nitrides with the general formula $M_{n+1}AX_n$ (where M is an early transition metal, A is a group 13–16 element, and X is carbon or nitrogen)—such as Ti_3SiC_2 and Cr_2AlC, or alumina-based feedstocks. Complex channel geometries—TPMS lattices, lung-inspired topologies, or multi-flow designs—achieve superior surface-to-volume ratios, heat-transfer coefficients, and thermal shock resistance compared to conventionally machined or cast counterparts. These structures withstand harsh environments (high-temperature corrosion, molten salts in concentrated solar power thermal energy storage, or industrial processes), offering leak-free operation and efficiencies unattainable by traditional methods. Recent demonstrations (2022–2025) include UHTC-based exchangers for concentrated solar power

and heating, ventilation, and air conditioning system, with densities (> 92%) and minimal distortion post-sintering. Structurally, EBAM enables lightweight, high-strength ceramic components (e.g., impellers, nozzles, or load-bearing lattices) with tailored porosity for filtration, catalysis, or insulation, combining mechanical reliability with thermal/chemical stability [151]. A compelling demonstration of EBAM's capability in large-scale structural marine energy components is illustrated in Figure 17. It shows carbon fiber tidal turbine rotors manufactured via EBAM for SIMEC© Atlantis Energy's AR1500® floating tidal energy system in Scotland, alongside the conceptual 3D design of a tidal blade section mold, highlighting the technique's potential for producing durable, high-performance parts in demanding marine environments [152,153].

9.5. Summary perspective

The application landscape of EBAM for polymer-ceramic composites and monolithic ceramics continues to expand rapidly, driven by its unparalleled ability to marry material functionality (biocompatibility, ultra-high-temperature stability, piezoelectric response, ionic conductivity) with geometric complexity (graded structures, internal channels, multi-material integration). Convergence of tailored microstructures, scalable feedstock development, and hybrid post-processing has overcome historical limitations in density, anisotropy, and resolution, delivering components with performance metrics rivaling or exceeding conventional routes. As feedstock versatility and printer capabilities advance—encompassing higher loadings, faster de‑binding, and AI-optimized designs—EBAM is poised to revolutionize high-performance engineering across biomedical personalization, aerospace extreme environments, smart electronics, sustainable energy systems, and beyond. Future directions include fully integrated multi-functional devices, in-situ monitoring, and sustainable (recycled or bio-derived) feedstocks, solidifying EBAM's role as a cornerstone of advanced manufacturing.

10.CONCLUSION

Extrusion-based additive manufacturing (EBAM) has emerged as a versatile and cost-effective platform for the fabrication of highly filled polymer-ceramic composites and, following appropriate post-processing, dense ceramic components. By enabling the extrusion of either highly loaded suspensions or thermoplastic filaments containing significant ceramic fractions, EBAM facilitates the layer-by-layer construction of complex geometries that are often unattainable using conventional manufacturing techniques.

The principal advantages of EBAM include relatively low equipment and processing costs, high flexibility in feedstock formulation, and the capability to achieve elevated ceramic loadings—frequently exceeding 50 vol.%—which is essential for attaining high-performance composites and near-fully dense ceramic structures. Depending on the application, printed parts may function directly as polymer-ceramic composites or undergo subsequent post-processing steps, such as photopolymerization (e.g., UV/IR curing in polymer-derived ceramics), thermal de‑binding, and high-temperature sintering, to obtain monolithic ceramic components with reduced porosity and enhanced mechanical integrity. However, several challenges still limit the widespread industrial adoption of EBAM. These include the need for precise control of rheological properties—particularly viscosity, yield stress, and shear-thinning behavior—along with ensuring homogeneous particle dispersion and mitigating defect formation such as cracking, warping, and interlayer delamination during drying and sintering. Furthermore, the optimization of processing parameters, including nozzle geometry, extrusion pressure, deposition rate, and layer height, remains essential for achieving consistent shape fidelity and robust interfacial bonding.

From a broader perspective, the performance of EBAM-fabricated materials is governed by a tightly coupled process–structure–property relationship, where rheological characteristics dictate printability, which in turn influences microstructural evolution and ultimately determines functional properties. Addressing this multi-scale interdependence requires integrated optimization strategies and the development of predictive models capable of linking material formulation to final performance. Looking forward, EBAM holds significant potential as a key enabling technology in advanced manufacturing sectors, including biomedical engineering, aerospace systems, thermal management, and structural ceramics. Future progress is expected to be driven by advances in feedstock engineering, real-time process monitoring, multi-material and multi-scale printing strategies, and the development of sustainable and high-performance binder systems. Such developments will be critical for bridging the gap between laboratory-scale demonstrations and reliable industrial applications.

REFERENCES

[1] M. Pelanconi, A. Ortona. Review on the design approaches of cellular architectures produced by additive manufacturing. In: M Meboldt, C. Klahn (Eds.). *Industrializing Additive Manufacturing. AMPA 2020.* Springer, Cham, 2021, pp. 52–64.

[2] A. Villa, P.K. Gianchandani, F. Baino. Sustainable approaches for the additive manufacturing of ceramic materials. *Ceramics*, 2024, vol. 7, no. 1, pp. 291–309.

[3] T.D. Ngo, A. Kashani, G. Imbalzano, K.T.Q. Nguyen, D. Hui. Additive manufacturing (3D printing): A review of

materials, methods, applications and challenges. *Composites Part B: Engineering*, 2018, vol. 143, pp. 172–196.
[4] R. Spina, L. Morfini. Material extrusion additive manufacturing of ceramics: A review on filament-based process. *Materials*, 2024, vol. 17, no. 11, art. no. 2779.
[5] A. Jaberi, E.N. Dresvyanina. Sustainable polymer composites from industrial wastes. *Reviews on Advanced Materials and Technologies*, 2025, vol. 7, no. 1, pp. 24–52.
[6] A. Patil, A. Patel, R. Purohit. An overview of polymeric materials for automotive applications. *Materials Today: Proceedings*, 2017, vol. 4, no. 2, pp. 3807–3815.
[7] H. Lipson, M. Kurman. *Fabricated: The New World of 3D Printing*. John Wiley & Sons, Inc., 2013, pp. 1–5.
[8] D. Espalin, D.W. Muse, E. MacDonald, R.B. Wicker. 3D printing multifunctionality: Structures with electronics. *International Journal of Advanced Manufacturing Technology*, 2014, vol. 72, no. 5–8, pp. 963–978.
[9] G. Saberi, A. Hadian, S. Mahboubizadeh, A. Asefnejad. Natural polymeric reinforcement during 3D-printing in bone regeneration. In: *The 12th International Conference on Materials Science & Metallurgical Engineering*, Tehran, 2023.
[10] I.L. de Camargo, C.A. Fortulan, H.A. Colorado. A review on the ceramic additive manufacturing technologies and availability of equipment and materials. *Ceramica*, 2022, vol. 68, no. 387, pp. 329–347.
[11] S.J. Rodrigues, R.P. Chartoff, D.A. Klosterman, M. Agarwala, N. Hecht. Solid freeform fabrication of functional silicon nitride ceramics by laminated object manufacturing. In: *International Solid Freeform Fabrication Symposium*, Austin, TX, USA, 2000.
[12] A. Zocca, J. Günster. LSD-based 3D printing of alumina ceramics. *Journal of Ceramic Science and Technology*, 2017, vol. 8, no. 1, pp. 141–148.
[13] Y. Lakhdar, C. Tuck, J. Binner, A. Terry, R. Goodridge. Additive manufacturing of advanced ceramic materials. *Progress in Materials Science*, 2021, vol. 116, art. no. 100736.
[14] S.B. Balani, S.H. Ghaffar, M. Chougan, E. Pei, E. Şahin. Processes and materials used for direct writing technologies: A review. *Results in Engineering*, 2021, vol. 11, art. no. 100257.
[15] V. Monfared, H.R. Bakhsheshi-Rad, S. Ramakrishna, M. Razzaghi, F. Berto. A brief review on additive manufacturing of polymeric composites and nanocomposites. *Micromachines*, 2021, vol. 12, no. 6, art. no. 704.
[16] U. Scheithauer, E. Schwarzer, H.J. Richter, T. Moritz. Thermoplastic 3D printing – An additive manufacturing method for producing dense ceramics. *International Journal of Applied Ceramic Technology*, 2015, vol. 12, no. 1, pp. 26–31.
[17] M.A. Roach, D. Keicher, E. Maines, B. Wall, C. Wall, J. Lavin, S. Whetten, L. Evans. Mechanical challenges of 3D printing ceramics using digital light processing. In: *International Solid Freeform Fabrication Symposium*, Austin, TX, USA, 2018.
[18] E.D. Lemma, B. Spagnolo, M. De Vittorio, F. Pisanello. Studying cell mechanobiology in 3D: The two-photon lithography approach. *Trends in Biotechnology*, 2018, vol. 37, no. 4, pp. 358–372.
[19] D.A. Klosterman, R.P. Chartoff, B. Priore, N. Osborne, G. Graves, A. Lightman, S.S. Pak, J. Weaver. Structural composites via laminated object manufacturing (LOM). In: *International Solid Freeform Fabrication Symposium*, Austin, TX, USA, 1996.
[20] N.R.F.A. Silva, L. Witek, P.G. Coelho, V.P. Thompson, E.D. Rekow, J. Smay. Additive CAD/CAM process for dental prostheses. *Journal of Prosthodontics*, 2011, vol. 20, no. 2, pp. 93–96.
[21] K. Rane, M. Strano. A comprehensive review of extrusion-based additive manufacturing processes for rapid production of metallic and ceramic parts. *International Journal of Advanced Manufacturing Technology*, 2019, vol. 7, no. 2, pp. 155–173.
[22] S. Lamnini, H. Elsayed, Y. Lakhdar, F. Baino, F. Smeacetto, E. Bernardo. Robocasting of advanced ceramics: Ink optimization and protocol to predict the printing parameters – A review. *Heliyon*, 2022, vol. 8, no. 9, art. no. e10651.
[23] W. Li, A. Armani, D. McMillen, M. Leu, G. Hilmas, J. Watts. Additive manufacturing of zirconia parts with organic sacrificial supports. *International Journal of Applied Ceramic Technology*, 2020, vol. 17, no. 4, pp. 1544–1553.
[24] A. Maguire, N. Pottackal, M.A.S.R. Saadi, M.M. Rahman, P.M. Ajayan. Additive manufacturing of polymer-based structures by extrusion technologies. *Oxford Open Materials Science*, 2021, vol. 1, no. 1, art. no. itaa004.
[25] T. Lacelle, K.L. Sampson, H. Yazdani Sarvestani, A. Rahimizadeh, J. Barroeta Robles, M. Mirkhalaf, M. Rafiee, M.B. Jakubinek, C. Paquet, B. Ashrafi. Additive manufacturing of polymer derived ceramics: Materials, methods, and applications. *APL Materials*, 2023, vol. 11, no. 7, art. no. 070602.
[26] A. Kulkarni, G.D. Sorarù, J.M. Pearce. Polymer-derived SiOC replica of material extrusion-based 3-D printed plastics. *Additive Manufacturing*, 2020, vol. 32, art. no. 100988.
[27] L.K. Tsui, E. Maines, L. Evans, D. Keicher, J. Lavin. Additive manufacturing of alumina components by extrusion of in-situ UV-cured pastes. In: *Proceedings of the 29th Annual International Solid Freeform Fabrication Symposium*, 2018, pp. 951–961.
[28] S. Tang, L. Yang, G. Li, X. Liu, Z. Fan. 3D printing of highly-loaded slurries via layered extrusion forming: Parameters optimization and control. *Additive Manufacturing*, 2019, vol. 28, pp. 546–553.
[29] J. Gonzalez-Gutierrez, S. Cano, S. Schuschnigg, C. Kukla, J. Sapkota, C. Holzer. Additive manufacturing of metallic and ceramic components by the material extrusion of highly-filled polymers: A review and future perspectives. *Materials*, 2018, vol. 11, no. 5, art. no. 840.
[30] F. Lebas, F. Marie, S. Marinel, C. Manière. A comparative study of CMC and HPMC binders for direct ink writing of ceramics. *Journal of the American Ceramic Society*, 2026, vol. 109, no. 2, art. no. e70565.
[31] K. Mitchell, W. Hua, E. Bandala, A.K. Gaharwar, Y. Jin. Particle–polymer interactions for 3D printing material design. *Chemical Physics Reviews*, 2024, vol. 5, no. 1, art. no. 011305.
[32] H. Hur, Y.J. Park, D.-H. Kim, J.W. Ko. Material extrusion for ceramic additive manufacturing with polymer-free ceramic precursor binder. *Materials & Design*, 2022, vol. 221, art. no. 110930.
[33] J. Gonzalez-Gutierrez, G.B. Stringari, B. Zupancic, G. Kubyshkina, B. Von Bernstorff, I. Emri. Time-dependent properties of multimodal polyoxymethylene based binder for powder injection molding. *Journal of Solid Mechanics and Materials Engineering*, 2012, vol. 6, no. 6, pp. 419–430.

[34] V. Tyagi, A. Thakur. Applications of biodegradable carboxymethyl cellulose-based composites. *Results in Materials*, 2023, vol. 20, art. no. 100481.
[35] P. Zhou, H. Qi, Z. Zhu, H. Qin, H. Li, C. Chu, M. Yan. Development of SiC/PVB composite powders for selective laser sintering additive manufacturing of SiC. *Materials*, 2018, vol. 11, no. 10, art. no. 2012.
[36] I. Oliver, J.A. Conesa, A. Fullana. Thermal decomposition of bio-based plastic materials. *Molecules*, 2024, vol. 29, no. 13, art. no. 3195.
[37] T. Yu, Z. Zhang, Q. Liu, R. Kuliiev, N. Orlovskaya, D. Wu. Extrusion-based additive manufacturing of yttria-partially-stabilized zirconia ceramics. *Ceramics International*, 2019, vol. 46, no. 4, pp. 5020–5027.
[38] A. Hadian, J. Duckek, A. Parrilli, A. Liersch, F. Clemens. Additive manufacturing of fiber-reinforced zirconia-toughened alumina ceramic matrix composites by material extrusion-based technology. *Advanced Engineering Materials*, 2024, vol. 26, no. 18, art. no. 2302158.
[39] E.F.C. Correa, E.A.T. Barahona, J.B.C. Castelló. Additive manufacturing of ceramic materials via direct ink writing (DIW): A review. *Ceramics*, 2026, vol. 9, no. 2, art. no. 16.
[40] S. Bhandari, P. Veteška, G. Vajpayee, M. Hinterstein, Ľ. Bača, Z. Hajdúchová, Z. Špitalský, G. Franchin, M. Janek. Material-extrusion based additive manufacturing of $BaTiO_3$ ceramics: From filament production to sintered properties. *Additive Manufacturing*, 2024, vol. 88, art. no. 104238.
[41] T.G. Aguirre, C.L. Cramer, D.J. Mitchell. Review of additive manufacturing and densification techniques for the net- and near net-shaping of geometrically complex silicon nitride components. *Journal of the European Ceramic Society*, 2021, vol. 42, no. 3, pp. 735–743.
[42] A. Goulas, B. Ozkan, A. Ketharam, S. Saremi-Yarahmadi, B. Vaidhyanathan. Additive manufacturing and characterisation of silicon carbide components fabricated using material extrusion-based fused filament fabrication. *Ceramics International*, 2025, vol. 51, no. 26, pp. 50779–50786.
[43] D. Ni, Y. Cheng, J. Zhang, J.-X. Liu, J. Zou, B. Chen, H. Wu, H. Li, S. Dong, J. Han, X. Zhang, Q. Fu, G.-J. Zhang. Advances in ultra-high temperature ceramics, composites, and coatings. *Journal of Advanced Ceramics*, 2021, vol. 11, no. 1, pp. 1–56.
[44] M.J. Zafar, D. Zhu, Z. Zhang. 3D printing of bioceramics for bone tissue engineering. *Materials*, 2019, vol. 12, no. 20, art. no. 3361.
[45] M. Thangavel, R.E. Selvam. Review of physical, mechanical, and biological characteristics of 3D-printed bioceramic scaffolds for bone tissue engineering applications. *ACS Biomaterials Science & Engineering*, 2022, vol. 8, no. 12, pp. 5060–5093.
[46] S. Whyman, K.M. Arif, J. Potgieter. Design and development of an extrusion system for 3D printing biopolymer pellets. *The International Journal of Advanced Manufacturing Technology*, 2018, vol. 96, no. 9–12, pp. 3417–3428.
[47] A. La Gala, R. Fiorio, M. Erkoç, L. Cardon, D.R. D'hooge. Theoretical evaluation of the melting efficiency for the single-screw micro-extrusion process: The case of 3D printing of ABS. *Processes*, 2020, vol. 8, no. 11, art. no. 1522.
[48] M. Fanous, S. Gold, S. Muller, S. Hirsch, J. Ogorka, G. Imanidis. Simplification of fused deposition modeling 3D-printing paradigm: Feasibility of 1-step direct powder printing for immediate release dosage form production. *International Journal of Pharmaceutics*, 2020, vol. 578, art. no. 119124.
[49] C.F. Guo, M. Zhang, B. Bhandari. A comparative study between syringe-based and screw-based 3D food printers by computational simulation. *Computers and Electronics in Agriculture*, 2019, vol. 162, pp. 397–404.
[50] A. Goyanes, N. Allahham, S.J. Trenfield, E. Stoyanov, S. Gaisford, A.W. Basit. Direct powder extrusion 3D printing: Fabrication of drug products using a novel single-step process. *International Journal of Pharmaceutics*, 2019, vol. 567, art. no. 118471.
[51] C.T. Joseph, T.A. Baer, P. Calvert. Recent developments in freeform fabrication of dense ceramics from slurry deposition. In: *International Solid Freeform Fabrication Symposium*, Austin, TX, USA, 1997.
[52] L.M. Rueschhoff, W.J. Costakis, M.J. Michie, J.P. Youngblood, R.W. Trice. Additive manufacturing of dense ceramic parts via direct ink writing of aqueous alumina suspensions. *International Journal of Applied Ceramic Technology*, 2016, vol. 13, no. 5, pp. 821–830.
[53] Q. Fu, E. Saiz, A.P. Tomsia. Direct ink writing of highly porous and strong glass scaffolds for load-bearing bone defects repair and regeneration. *Acta Biomaterialia*, 2011, vol. 7, no. 10, pp. 3547–3554.
[54] M.C. Leu, L. Tang, B.K. Deuser, R.G. Landers, G. Hilmas, S.C. Zhang, J.L. Watts. Freeze-form extrusion fabrication of composite structures. In: *22nd Annual International Solid Freeform Fabrication Symposium*, Austin, TX, USA, 2011, pp. 111–124.
[55] T. Schlordt, S. Schwanke, F. Keppner, T. Fey, N. Travitzky, P. Greil. Robocasting of alumina hollow filament lattice structures. *Journal of the European Ceramic Society*, 2013, vol. 33, no. 15–16, pp. 3243–3248.
[56] W.J. Costakis, L.M. Rueschhoff, A.I. Diaz-Cano, J.P. Youngblood, R.W. Trice. Additive manufacturing of boron carbide via continuous filament direct ink writing of aqueous ceramic suspensions. *Journal of the European Ceramic Society*, 2016, vol. 36, no. 14, pp. 3249–3256.
[57] F.J. Martínez-Vázquez, A. Pajares, P. Miranda. A simple graphite-based support material for robocasting of ceramic parts. *Journal of the European Ceramic Society*, 2017, vol. 38, no. 4, pp. 2247–2250.
[58] M. Acosta, V.L. Wiesner, C.J. Martinez, R.W. Trice, J.P. Youngblood. Effect of polyvinylpyrrolidone additions on the rheology of aqueous, highly loaded alumina suspensions. *Journal of the American Ceramic Society*, 2013, vol. 96, no. 5, pp. 1372–1382.
[59] S.S. Nadkarni, J.E. Smay. Concentrated barium titanate colloidal gels prepared by bridging flocculation for use in solid freeform fabrication. *Journal of the American Ceramic Society*, 2006, vol. 89, no. 1, pp. 96–103.
[60] A. Marnot, A. Dobbs, B. Brettmann. Material extrusion additive manufacturing of dense pastes consisting of macroscopic particles. *MRS Communications*, 2022, vol. 12, no. 5, pp. 483–494.
[61] L.C. Hwa, S. Rajoo, A.M. Noor, N. Ahmad, M.B. Uday. Recent advances in 3D printing of porous ceramics: A review. *Current Opinion in Solid State and Materials Science*, 2017, vol. 21, no. 6, pp. 323–347.
[62] J.A. Lewis, J.E. Smay, J. Stuecker, J. Cesarano III. Direct ink writing of three-dimensional ceramic structures. *Journal of the American Ceramic Society*, 2006, vol. 89, no. 12, pp. 3599–3609.
[63] M. Mohammadi, P. Pascaud-Mathieu, V. Allizond, J.-M. Tulliani, B. Coppola, G. Banche, C. Chaput, A.M. Cuf-

fini, F. Rossignol, P. Palmero. Robocasting of single and multi-functional calcium phosphate scaffolds and its hybridization with conventional techniques: Design, fabrication and characterization. *Applied Sciences*, 2020, vol. 10, no. 23, art. no. 8677.

[64] L. Čelko, V. Gutiérrez-Cano, M. Casas-Luna, J. Matula, C. Oliver-Urrutia, M. Remešová, K. Dvořák, T. Zikmund, J. Kaiser, E.B. Montufar. Characterization of porosity and hollow defects in ceramic objects built by extrusion additive manufacturing. *Additive Manufacturing*, 2021, vol. 47, art. no. 102272.

[65] L. Wahl, M. Lorenz, J. Biggemann, N. Travitzky. Robocasting of reaction bonded silicon carbide structures. *Journal of the European Ceramic Society*, 2019, vol. 39, no. 15, pp. 4520–4526.

[66] J. Smay, J. Cesarano III, J.A. Lewis. Colloidal inks for directed assembly of 3-D periodic structures. *Langmuir*, 2002, vol. 18, no. 14, pp. 5429–5437.

[67] B.A. Tuttle, J.E. Smay, J. Cesarano III, J.A. Voigt, T.W. Scofield, W.R. Olson, J.A. Lewis. Robocast $Pb(Zr_{0.95}Ti_{0.05})O_3$ ceramic monoliths and composites. *Journal of the American Ceramic Society*, 2001, vol. 84, no. 4, pp. 872–874.

[68] E. Feilden, E. García-Tuñón, F. Giuliani, E. Saiz, L. Vandeperre. Robocasting of structural ceramic parts with hydrogel inks. *Journal of the European Ceramic Society*, 2016, vol. 36, no. 10, pp. 2525–2533.

[69] Y. Xia, Z. Lu, J. Cao, K. Miao, J. Li, D. Li. Microstructure and mechanical property of Cf/SiC core/shell composite fabricated by direct ink writing. *Scripta Materialia*, 2019, vol. 165, pp. 84–88.

[70] J.W. Kemp, N.S. Hmeidat, B.G. Compton. Boron nitride-reinforced polysilazane-derived ceramic composites via direct-ink writing. *Journal of the American Ceramic Society*, 2020, vol. 103, no. 8, pp. 4043–4050.

[71] H. Shao, X. Yang, Y. He, J. Fu, L. Liu, L. Ma, L. Zhang, G. Yang, C. Gao, Z. Gou. Bioactive glass-reinforced bioceramic ink writing scaffolds: Sintering, microstructure and mechanical behavior. *Biofabrication*, 2015, vol. 7, no. 3, art. no. 035010.

[72] L. Yang, X. Zeng, A. Ditta, B. Feng, L. Su, Y. Zhang. Preliminary 3D printing of large inclined-shaped alumina ceramic parts by direct ink writing. *Journal of Advanced Ceramics*, 2020, vol. 9, no. 3, pp. 312–319.

[73] C. Okyay, B. Sağbaş. Determining optimal robocasting process parameters for additive manufacturing of ceramic parts. *International Journal of 3D Printing Technologies and Digital Industry*, 2021, vol. 5, no. 3, pp. 435–444.

[74] R. Vaidyanathan, J. Walish, J.L. Lombardi, S. Kasichainula, P. Calvert, K.C. Cooper. Extrusion freeforming of functional ceramic prototypes. *JOM*, 2000, vol. 52, no. 12, pp. 34–37.

[75] A. Ghazanfari, W. Li, M.C. Leu, G.E. Hilmas. A novel freeform extrusion fabrication process for producing solid ceramic components with uniform layered radiation drying. *Additive Manufacturing*, 2017, vol. 15, pp. 102–112.

[76] A. Gómez-Gómez, J.J. Moyano, M.I. Osendi, M. Belmonte, P. Miranzo. The effect of rod orientation on the strength of highly porous filament printed 3D SiC ceramic architectures. *Boletín de la Sociedad Española de Cerámica y Vidrio*, 2020, vol. 60, no. 2, pp. 119–127.

[77] H. Zhang, Y. Yang, B. Liu, Z. Huang. The preparation of SiC-based ceramics by one novel strategy combined 3D printing technology and liquid silicon infiltration process. *Ceramics International*, 2019, vol. 45, no. 8, pp. 10800–10804.

[78] M.S. McClain, I.E. Gunduz, S.F. Son. Additive manufacturing of ammonium perchlorate composite propellant with high solids loadings. *Proceedings of the Combustion Institute*, 2019, vol. 37, no. 3, pp. 3135–3142.

[79] T. Huang, M.S. Mason, G.E. Hilmas, M.C. Leu. Freeze-form extrusion fabrication of ceramic parts. *Virtual and Physical Prototyping*, 2006, vol. 1, no. 2, pp. 93–100.

[80] X. Zhao. *Modeling and control of freeze-form extrusion fabrication*. M.S. thesis, Dept. Mechanical Engineering, University of Missouri–Rolla, Rolla, MO, USA, 2007.

[81] M.C. Leu, D.A. Garcia. Development of freeze-form extrusion fabrication with use of sacrificial material. *Journal of Manufacturing Science and Engineering*, 2014, vol. 136, no. 6, art. no. 061006.

[82] M.P. Serdeczny, R. Comminal, D.B. Pedersen, J. Spangenberg. Experimental and analytical study of the polymer melt flow through the hot-end in material extrusion additive manufacturing. *Additive Manufacturing*, 2020, vol. 32, art. no. 100997.

[83] M.C. Leu, B.K. Deuser, L. Tang, R.G. Landers, G.E. Hilmas, J.L. Watts. Freeze-form extrusion fabrication of functionally graded materials. *CIRP Annals*, 2012, vol. 61, no. 1, pp. 223–226.

[84] P. Gonzalez, E. Schwarzer, U. Scheithauer, N. Kooijmans, T. Moritz. Additive manufacturing of functionally graded ceramic materials by stereolithography. *Journal of Visualized Experiments*, 2019, no. 143, art. no. e57943.

[85] X. Ren, H. Shao, T. Lin, H. Zheng. 3D gel-printing—An additive manufacturing method for producing complex shape parts. *Materials & Design*, 2016, vol. 101, pp. 80–87.

[86] S. Park, W. Shou, L. Makatura, W. Matusik, K. Fu. 3D printing of polymer composites: Materials, processes, and applications. *Matter*, 2022, vol. 5, no. 1, pp. 43–76.

[87] A. Mahmood, F. Perveen, S. Chen, T. Akram, A. Irfan. Polymer composites in 3D/4D printing: Materials, advances, and prospects. *Molecules*, 2024, vol. 29, no. 2, art. no. 319.

[88] M. Mahmoudi, C. Wang, S. Moreno, S.R. Burlison, D. Alatalo, F. Hassanipour, S.E. Smith, M. Naraghi, M. Minary-Jolandan. Three-dimensional printing of ceramics through "carving" a gel and "filling in" the precursor polymer. *ACS Applied Materials & Interfaces*, 2020, vol. 12, no. 28, pp. 31984–31991.

[89] W. Li, A. Armani, A. Martin, B. Kroehler, A. Henderson, T. Huang, J. Watts, G. Hilmas, M. Leu. Extrusion-based additive manufacturing of functionally graded ceramics. *Journal of the European Ceramic Society*, 2021, vol. 41, no. 3, pp. 2049–2057.

[90] F. Hu, T. Mikolajczyk, D.Y. Pimenov, M.K. Gupta. Extrusion-based 3D printing of ceramic pastes: Mathematical modeling and in situ shaping retention approach. *Materials*, 2021, vol. 14, no. 5, art. no. 1137.

[91] A. Ghazanfari, W. Li, M.C. Leu, G.E. Hilmas. A novel extrusion-based additive manufacturing process for ceramic parts. In: *Proceedings of the 27th Annual International Solid Freeform Fabrication Symposium*, Austin, TX, USA, 2016, pp. 1509–1529.

[92] J.A. Lewis. Colloidal processing of ceramics. *Journal of the American Ceramic Society*, 2000, vol. 83, no. 10, pp. 2341–2359.

[93] L. Rueschhoff. *Ceramic near-net shaped processing using highly-loaded aqueous suspensions*. Ph.D. dissertation, Purdue University, West Lafayette, IN, USA, 2017.

[94] D. McMillen, W. Li, M.-C. Leu, G. Hilmas. Designed extrudate for additive manufacturing of zirconium diboride by ceramic on-demand extrusion. In: *Proceedings of the 27th Annual International Solid Freeform Fabrication Symposium*, Austin, TX, USA, 2016, pp. 929–938.

[95] S.C. Altıparmak, V.A. Yardley, Z. Shi, J. Lin. Extrusion-based additive manufacturing technologies: State of the art and future perspectives. *Journal of Manufacturing Processes*, 2022, vol. 83, pp. 607–636.

[96] F. Clemens, F. Sarraf, A. Borzì, A. Neels, A. Hadian. Material extrusion additive manufacturing of advanced ceramics: Towards the production of large components. *Journal of the European Ceramic Society*, 2023, vol. 43, no. 7, pp. 2752–2760.

[97] M.R. Condruz, A. Paraschiv, T.-A. Badea, D. Useriu, T.-F. Frigioescu, G. Badea, G. Cican. A study on mechanical properties of low-cost thermoplastic-based materials for material extrusion additive manufacturing. *Polymers*, 2023, vol. 15, no. 14, art. no. 2981.

[98] S. Cailleaux, N.M. Sanchez-Ballester, Y.A. Gueche, B. Bataille, I. Soulairol. Fused deposition modeling (FDM), the new asset for the production of tailored medicines. *Journal of Controlled Release*, 2020, vol. 330, pp. 821–841.

[99] N. Dumpa, A. Butreddy, H. Wang, N. Komanduri, S. Bandari, M.A. Repka. 3D printing in personalized drug delivery: An overview of hot-melt extrusion-based fused deposition modeling. *International Journal of Pharmaceutics*, 2021, vol. 600, art. no. 120501.

[100] C. Parulski, O. Jennotte, A. Lechanteur, B. Evrard. Challenges of fused deposition modeling 3D printing in pharmaceutical applications: Where are we now? *Advanced Drug Delivery Reviews*, 2021, vol. 175, art. no. 113810.

[101] A. Melocchi, F. Briatico-Vangosa, M. Uboldi, F. Parietti, M. Turchi, D. von Zeppelin, A. Maroni, L. Zema, A. Gazzaniga, A. Zidan. Quality considerations on the pharmaceutical applications of fused deposition modeling 3D printing. *International Journal of Pharmaceutics*, 2020, vol. 592, art. no. 119901.

[102] M.K. Agarwala, R. Van Weeren, A. Bandyopadhyay, P.J. Whalen, A. Safari, S.C. Danforth. Fused deposition of ceramics and metals: An overview. In: *International Solid Freeform Fabrication Symposium*, Austin, TX, USA, 1995.

[103] A. Jaberi, A. Alimohammadi, S. Mahboubizadeh, E.N. Dresvyanina. Advanced multifunctional composite cellular structures: Innovations and impact in aerospace engineering. *Reviews on Advanced Materials and Technologies*, 2025, vol. 7, no. 3, pp. 155–183.

[104] J. Macedo, A. Samaro, V. Vanhoorne, C. Vervaet, J.F. Pinto. Processability of poly(vinyl alcohol) based filaments with paracetamol prepared by hot-melt extrusion for additive manufacturing. *Journal of Pharmaceutical Sciences*, 2020, vol. 109, no. 12, pp. 3636–3644.

[105] A. Samaro, P. Janssens, V. Vanhoorne, J. Van Renterghem, M. Eeckhout, L. Cardon, T. De Beer, C. Vervaet. Screening of pharmaceutical polymers for extrusion-based additive manufacturing of patient-tailored tablets. *International Journal of Pharmaceutics*, 2020, vol. 586, art. no. 119591.

[106] S.J. Trenfield, A. Awad, A. Goyanes, S. Gaisford, A.W. Basit. 3D printing pharmaceuticals: Drug development to frontline care. *Trends in Pharmacological Sciences*, 2018, vol. 39, no. 5, pp. 440–451.

[107] H. Gong, D. Snelling, K. Kardel, A. Carrano. Comparison of stainless steel 316L parts made by FDM- and SLM-based additive manufacturing processes. *JOM*, 2019, vol. 71, no. 3, pp. 880–885.

[108] M.K. Agarwala, A. Bandyopadhyay, R. Van Weeren, N.A. Langrana, A. Safari, S.C. Danforth, V.R. Jamalabad, P.J. Whalen, R. Donaldson, J. Pollinger. Fused deposition of ceramics (FDC) for structural silicon nitride components. In: *International Solid Freeform Fabrication Symposium*, Austin, TX, USA, 1995.

[109] E. Fuenmayor, M. Forde, A.V. Healy, D.M. Devine, J.G. Lyons, C. McConville, I. Major. Material considerations for fused-filament fabrication of solid dosage forms. *Pharmaceutics*, 2018, vol. 10, no. 2, art. no. 44.

[110] P. Xu, J. Li, A. Meda, F. Osei-Yeboah, M.L. Peterson, M.A. Repka, X. Zhan. Development of a quantitative method to evaluate the printability of filaments for fused deposition modeling 3D printing. *International Journal of Pharmaceutics*, 2020, vol. 588, art. no. 119760.

[111] J. Aho, J.P. Bøtker, N. Genina, M. Edinger, L. Arnfast, J. Rantanen. Roadmap to 3D-printed oral pharmaceutical dosage forms: Feedstock filament properties and characterization for fused deposition modeling. *Journal of Pharmaceutical Sciences*, 2018, vol. 108, no. 1, pp. 26–35.

[112] B. Shaqour, M. Abuabiah, S. Abdel-Fattah, A. Juaidi, R. Abdallah, W. Abuzaina, M. Qarout, B. Verleije, P. Cos. Gaining a better understanding of the extrusion process in fused filament fabrication 3D printing: A review. *International Journal of Advanced Manufacturing Technology*, 2021, vol. 114, no. 5–6, pp. 1279–1291.

[113] H. Masuda, Y. Ohta, M. Kitayama. Additive manufacturing of SiC ceramics with complicated shapes using the FDM type 3D-printer. *Journal of Materials Science and Chemical Engineering*, 2019, vol. 07, no. 2, pp. 1–12.

[114] E.L. Scheller, P.H. Krebsbach, D.H. Kohn. Robocasting and mechanical testing of aqueous silicon nitride slurries. *Journal of Oral Rehabilitation*, 2009, vol. 36, no. 5, pp. 368–389.

[115] U. Scheithauer, E. Schwarzer, C. Poitzsch, H.-J. Richter, T. Moritz, M. Stelter. *Method for producing ceramic and/or metal components*. U.S. Patent Application US20170182554A1, issued Jun. 29, 2017.

[116] R. He, N. Zhou, K. Zhang, X. Zhang, L. Zhang, W. Wang, D. Fang. Progress and challenges towards additive manufacturing of SiC ceramic. *Journal of Advanced Ceramics*, 2021, vol. 10, no. 4, pp. 637–674.

[117] U. Scheithauer, J. Pötschke, S. Weingarten, E. Schwarzer, A. Vornberger, T. Moritz, A. Michaelis. Droplet-based additive manufacturing of hard metal components by thermoplastic 3D printing (T3DP). *Journal of Ceramic Science and Technology*, 2017, vol. 8, no. 1, pp. 155–160.

[118] A.D. Valino, J.R.C. Dizon, A.H. Espera, Q. Chen, J. Messman, R.C. Advincula. Advances in 3D printing of thermoplastic polymer composites and nanocomposites. *Progress in Polymer Science*, 2019, vol. 98, art. no. 101162.

[119] A. Marnot, K. Koube, S. Jang, N. Thadhani, J. Kacher, B. Brettmann. Material extrusion additive manufacturing of high particle loaded suspensions: A review of materials, processes and challenges. *Virtual and Physical Prototyping*, 2023, vol. 18, no. 1, art. no. e2279149.

[120] O. Bouzaglou, O. Golan, N. Lachman. Process design and parameters interaction in material extrusion 3D printing: A review. *Polymers*, 2023, vol. 15, no. 10, art. no. 2280.

[121] C. Petit, C. Meunier, L. Manceaux, H. Rivera, H. Taxil. Fused deposition modeling and microwave sintering of 3Y-TZP samples. *Open Ceramics*, 2023, vol. 15, art. no. 100378.

[122] R. Brucculeri, L. Airoldi, P. Baldini, B. Vigani, S. Rossi, S. Morganti, F. Auricchio, U. Anselmi-Tamburini. Spark plasma sintering of complex metal and ceramic structures produced by material extrusion. *3D Printing and Additive Manufacturing*, 2023, vol. 11, no. 3, pp. 1246–1256.

[123] F.C. Nunes, P.A. Lançoni, G.H.M. Gomes, K.F. Santos, E.Y. Nagata, J.V. Campos, I.C.F. Moraes, J.K.M.B. Daguano, E.M.J.A. Pallone. Flash sintering of 3D-printed 3YSZ scaffolds for bone tissue engineering. *Ceramics International*, 2025, vol. 51, no. 13, pp. 17704–17717.

[124] P. Gkertzos, A. Kotzakolios, G. Mantzouranis, V. Kostopoulos. Nozzle temperature calibration in 3D printing. *International Journal of Interactive Design and Manufacturing*, 2024, vol. 18, no. 2, pp. 879–899.

[125] N. Vidakis, M. Petousis, J.D. Kechagias. A comprehensive investigation of the 3D printing parameters' effects on the mechanical response of polycarbonate in fused filament fabrication. *Progress in Additive Manufacturing*, 2022, vol. 7, no. 4, pp. 713–722.

[126] Z. Fu, V. Angeline, W. Sun. Evaluation of printing parameters on 3D extrusion printing of pluronic hydrogels and machine learning guided parameter recommendation. *International Journal of Bioprinting*, 2021, vol. 7, no. 4, art. no. 434.

[127] T. Rijwani, P. Ramkumar. Thermal debinding for binder burnout in metal and ceramic processing. *Heat Transfer Engineering*, 2024, vol. 46, no. 7, pp. 615–626.

[128] S. Cano, J. Gonzalez-Gutierrez, J. Sapkota, M. Spoerk, F. Arbeiter, S. Schuschnigg, C. Holzer, C. Kukla. Additive manufacturing of zirconia parts by fused filament fabrication and solvent debinding: Selection of binder formulation. *Additive Manufacturing*, 2019, vol. 26, pp. 117–128.

[129] Z. Lotfizarei, A. Mostafapour, A. Barari, A. Jalili, A.E. Patterson. Overview of debinding methods for parts manufactured using powder material extrusion. *Additive Manufacturing*, 2022, vol. 61, art. no. 103335.

[130] S. Bhandari, C. Manière, F. Sedona, E. De Bona, V.M. Sglavo, P. Colombo, L. Fambri, M. Biesuz, G. Franchin. Ultra-rapid debinding and sintering of additively manufactured ceramics by ultrafast high-temperature sintering. *Journal of the European Ceramic Society*, 2023, vol. 44, no. 1, pp. 328–340.

[131] J. Ghorbani, P. Koirala, Y.-L. Shen, M. Tehrani. Eliminating voids and reducing mechanical anisotropy in fused filament fabrication parts by adjusting the filament extrusion rate. *Journal of Manufacturing Processes*, 2022, vol. 80, pp. 651–658.

[132] M. Spoerk, J. Sapkota, G. Weingrill, T. Fischinger, F. Arbeiter, C. Holzer. Shrinkage and warpage optimization of expanded-perlite-filled polypropylene composites in extrusion-based additive manufacturing. *Macromolecular Materials and Engineering*, 2017, vol. 302, no. 10, art. no. 1700143.

[133] S. Bose, E.K. Akdogan, V.K. Balla, S. Ciliveri, P. Colombo, G. Franchin, N. Ku, P. Kushram, F. Niu, J. Pelz, A. Rosenberger, A. Safari, Z. Seeley, R.W. Trice, L. Vargas-Gonzalez, J.P. Youngblood, A. Bandyopadhyay. 3D printing of ceramics: Advantages, challenges, applications, and perspectives. *Journal of the American Ceramic Society*, 2024, vol. 107, no. 12, pp. 7879–7920.

[134] M. Dadkhah, J.-M. Tulliani, A. Saboori, L. Iuliano. Additive manufacturing of ceramics: Advances, challenges, and outlook. *Journal of the European Ceramic Society*, 2023, vol. 43, no. 15, pp. 6635–6664.

[135] A. Challapalli, G. Li. *Artificial Intelligence Assisted Structural Optimization*. CRC Press, 2025.

[136] P. González-Suárez, P.M. Hernández-Castellano, A. Narganes-Pineda. Additive manufacturing of ceramics study: Sustainable material extrusion and its potential role in circular economy. *Applied Sciences*, 2026, vol. 16, no. 2, art. no. 1019.

[137] N.R. Mehrabadi, G. Pircheraghi, A. Ghasemkhani, P.H. Sanati, A. Shahidizadeh, A. Kaviani, S. Sinha Ray. A review on material extrusion additive manufacturing of polycarbonate-based blends and composites: Process–structure–property relationships. *SPE Polymers*, 2025, vol. 6, no. 2, art. no. e10174.

[138] H. Wang, B. Han, P. Zheng, Z. Liu, Q. Zhang. Recent advances of defect-driven hybrid additive manufacturing of extrusion-based polymers: Bridging multiscale mechanisms to enhanced structural performance. *Advanced Composites and Hybrid Materials*, 2026, vol. 9, no. 1, art. no. 46.

[139] Z.L. Li, S. Zhou, E. Saiz, R. Malik. Ink formulation in direct ink writing of ceramics: A meta-analysis. *Journal of the European Ceramic Society*, 2024, vol. 44, no. 12, pp. 6777–6796.

[140] S. Khuje, N. Ku, A. Bujanda, J. Yu, H. Tsang, N. Meuse, L. Vargas-Gonzalez, S. Ren. Additive manufacturing pathways for polymer-derived ceramics: Processing, structure, and function. *npj Advanced Manufacturing*, 2026, vol. 3, no. 1, art. no. 8.

[141] V. Bishop, S.C. Mathur, N. Nguyen, B. Sharma, M. Drouin, B. Li, C. Park, W. Wei. A review of direct ink writing of polymer-derived ceramics. *Virtual and Physical Prototyping*, 2025, vol. 20, no. 1, art. no. 2499938.

[142] Y. Li, A. Chen, J. Su, Y. Li, Y. Zhang, Z. Li, S. Zhou, J. He, Z. Cao, Y. Shi, J. Lu, C. Yan. An overview on ceramic multi-material additive manufacturing: Progress and challenges. *International Journal of Extreme Manufacturing*, 2025, vol. 7, no. 4, art. no. 042005.

[143] A. Dedeloudi, P.M. Bertelli, L. Martinez-Marcos, T. Quinten, I. Lengyel, S.K. Andersen, D.A. Lamprou. Development of bioceramic bone-inspired scaffolds through single-step melt-extrusion 3D printing for segmental defect treatment. *Journal of Functional Biomaterials*, 2025, vol. 16, no. 10, art. no. 358.

[144] N.J. Lores, B. Aráoz, X. Hung, M.H. Talou, A.R. Boccaccini, G.A. Abraham, É.B. Hermida, P.C. Caracciolo. 3D-printed poly(ester urethane)/poly(3-hydroxybutyrate-co-3-hydroxyvalerate)/bioglass scaffolds for tissue engineering applications. *Polymers*, 2024, vol. 16, no. 23, art. no. 3355.

[145] M.A. Alghauli, A.Y. Alqutaibi, S. Wille, M. Kern. The physical-mechanical properties of 3D-printed versus conventional milled zirconia for dental clinical applications: A systematic review with meta-analysis. *Journal of the Mechanical Behavior of Biomedical Materials*, 2024, vol. 156, art. no. 106601.

[146] D. Lipke. *UHT-CAMANCHE: Ultra-high temperature ceramic additively manufactured compact heat exchangers*. Technical Report, 2024.

[147] C. Shen, Y. Guo, Z. Shen, F. Yan, N. Zhong. Additive manufacturing of aerospace composites: A critical review of the material–process–design interplay and prospects for application. *Materials*, 2025, vol. 18, no. 18, art. no. 4280.

[148] T. Rosental, G. Gatani, C.F. Pirri, C. Ricciardi, D. Savraeva, A. Bunin, M.Y. Moshkovitz-Douvdevany, S. Magdassi, S. Stassi. Unlocking enhanced piezoelectric performance

through 3D printing of particle-free ceramic piezoelectric complex structures and metamaterials. *Chemical Engineering Journal*, 2024, vol. 499, art. no. 156189.
[149] R.S. Govindarajan, Z. Ren, I. Melendez, S.K.S. Boetcher, F. Madiyar, D. Kim. Polymer nanocomposite sensors with improved piezoelectric properties through additive manufacturing. *Sensors*, 2024, vol. 24, no. 9, art. no. 2694.
[150] S. Masciandaro, M. Torrell, P. Leone, A. Tarancón. Three-dimensional printed yttria-stabilized zirconia self-supported electrolytes for solid oxide fuel cell applications. *Journal of the European Ceramic Society*, 2017, vol. 39, no. 1, pp. 9–16.
[151] E. Tabares, M. Kitzmantel, E. Neubauer, A. Jimenez-Morales, S.A. Tsipas. Extrusion-based additive manufacturing of Ti_3SiC_2 and Cr_2AlC MAX phases as candidates for high temperature heat exchangers. *Journal of the European Ceramic Society*, 2021, vol. 42, no. 3, pp. 841–849.
[152] L. Palmer, D. Gillespie, J.D.J. MacAulay, C.E. Sparling, D.J.F. Russell, G.D. Hastie. Harbour porpoise (Phocoena phocoena) presence is reduced during tidal turbine operation. *Aquatic Conservation: Marine and Freshwater Ecosystems*, 2021, vol. 31, no. 12, pp. 3543–3553.
[153] P. Murdy, J. Dolson, D. Miller, S. Hughes, R. Beach. Leveraging the advantages of additive manufacturing to produce advanced hybrid composite structures for marine energy systems. *Applied Sciences*, 2021, vol. 11, no. 3, art. no. 1336.

УДК 778.64

Аддитивное производство на основе экструзии полимер-керамических композитов и керамических компонентов с использованием высоконаполненных фидстоков: обзор

Ш. Махбубизаде [1], А. Джабери [2], Е.Н. Дресвянина [2], А. Тахерхани [3], Ш. Ашури [3]

[1] Кафедра материаловедения и инженерии, Исламский (Азад) университет, Научно-исследовательский кампус, Тегеран, 1477893855, Иран
[2] Институт текстиля и моды, Санкт-Петербургский государственный университет промышленных технологий и дизайна, ул. Большая Морская, д. 18, Санкт-Петербург, 191186, Россия
[3] Кафедра инженерии, Исламский (Азад) университет, Научно-исследовательский кампус, Тегеран, 1477893855, Иран

Аннотация. Аддитивное производство на основе экструзии стало мощной технологией для изготовления полимер-керамических композитов со сложной геометрией. Благодаря послойному нанесению материала без необходимости в формах этот процесс значительно снижает отходы материалов и производственные затраты, особенно при мелкосерийном и индивидуальном производстве. Среди различных технологий аддитивного производства методы на основе экструзии (экструзионная 3D-печать) получили широкое распространение благодаря своей экономичности, гибкости проектирования и совместимости с широким спектром материалов. Эти процессы обычно используют полимеры в качестве связующих или матриц в сочетании с высокой загрузкой керамических порошков и функциональных добавок, при этом керамическая фаза играет доминирующую роль в формировании конечных механических, термических и функциональных свойств изделия. Настоящий обзор представляет собой всесторонний анализ аддитивного производства на основе экструзии полимер-керамических композитов. В нём систематически рассматриваются ключевые системы материалов, составы связующих, технологические маршруты, стратегии постобработки, а также критические параметры, определяющие развитие микроструктуры и общие эксплуатационные характеристики.

Ключевые слова: аддитивное производство; полимерные композиты; керамический порошок; экструзия; 3D-печать